Chapter 8 Generalized Conforming Thick Plate Element

Song Cen
Department of Engineering Mechanics, School of Aerospace,
Tsinghua University, Beijing, 100084, China

Zhi-Fei Long
School of Mechanics & Civil Engineering, China University of
Mining & Technology, Beijing, 100083, China

Abstract This chapter introduces how to use the generalized conforming theory to develop the plate element models for the analysis of both thick and thin plates. In Sects. 8.1 and 8.2, a review of the Reissner-Mindlin (thick) plate theory is firstly given, and then, a comparison between this theory and the Kirchhoff (thin) plate theory is presented. In the subsequent sections, the construction methods for the thick/thin plate elements are firstly summarized; especially, the shear locking difficulty caused by the traditional scheme (assuming deflection and rotation fields) is analyzed. Then, three new schemes which are proposed by the authors and can eliminate shear locking from the outset are introduced in detail, including the schemes of assuming rotation and shear strain fields, assuming deflection and shear strain fields, and introducing the shear strain field into the thin plate elements. The formulations of four triangular and rectangular element models are also presented. Numerical examples show that the proposed models exhibit excellent performance for both thick and thin plates, and no shear locking happens.

Keywords thick plate element, generalized conforming, Reissner-Mindlin (thick) plate theory, thick/thin beam element, shear locking.

8.1 Summary of the Thick Plate Theory

The thick plates discussed here is restricted to moderately-thick plates. Limitation will appear if classical thin plate theory is used to analyze such thick plates.

The fundamental equations of the thick plate theory were firstly proposed by Reissner in the forties of the twentieth century[1].

Compared with the thin plate theory, the main characteristic of the thick plate theory is that it considers the influences of the transverse shear strain γ_{xz} and γ_{yz} (hereafter referred to as γ_x and γ_y). So, the thick plate theory is also called the shear deformation plate bending theory. Furthermore, in dynamics problems, the influences of rotatory inertia should also be considered[2].

In the thick plate theory, the shear strain can be expressed in terms of the deflection w and the normal slopes ψ_x and ψ_y as

$$\gamma_x = \frac{\partial w}{\partial x} - \psi_x, \quad \gamma_y = \frac{\partial w}{\partial y} - \psi_y \tag{8-1}$$

in which w, ψ_x, ψ_y are three independent generalized displacements. On the contrary, in the thin plate theory, since γ_x and γ_y are assumed to be zero, Eq. (8-1) will degenerate to be

$$\psi_x = \frac{\partial w}{\partial x}, \quad \psi_y = \frac{\partial w}{\partial y} \tag{8-2}$$

Only one independent displacement w exists, and both ψ_x and ψ_y depend on w. Therefore, the thick plate theory is also called the plate bending theory with three generalized displacements[3].

Owing to constructional reason, the shear deformation of sandwich plates cannot be ignored. So, the thick plate theory can be used to calculate the sandwich plate problems. Furthermore, it is more reasonable to employ the thick plate theory to analyze the following problems: high-order vibration problem of plates, stress concentration problem, stress distribution problem near free edges, contact problem[3].

This section compendiously gives the fundamental equations of the thick plate theory, including equilibrium equations, geometrical equations, physical equations, coordinate transformations, boundary conditions, expressions of strain energy and strain complementary energy. For these fundamental equations of the thick plate theory, it is necessary to emphatically understand the difference from those in the thin plate theory and the influence of shear deformation.

8.1.1 Equilibrium Equations

A thick plate in Cartesian coordinates (x, y, z) is shown in Fig. 8.1. The x and y co-ordinates are in the reference middle surface; z is the co-ordinate through the thickness h, and its positive direction is upward.

The load density on the middle surface has three components q, m_x and m_y, in which q is the load density along the z-axis, and its positive direction is also upward; m_x is the couple load density in the xz-plane, and its positive direction is the same

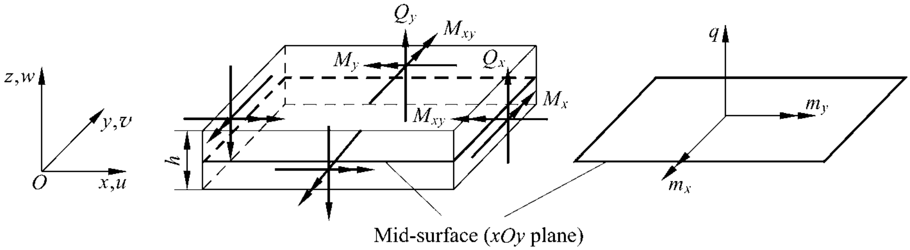

Figure 8.1 The coordinates, internal forces and load density components used in thick plate bending problem

as the rotation from x-axis to z-axis; m_y is the couple load density in the yz-plane, and its positive direction is the same as the rotation from y-axis to z-axis.

In the Cartesian coordinate system, the moderately thick plate has 5 internal force components: bending moments M_x and M_y, twisting moment $M_{xy} = M_{yx}$, transverse shear forces Q_x and Q_y. And, their positive directions are shown in Fig. 8.1. These 5 components can form an internal force vector:

$$\boldsymbol{S} = [M_x \quad M_y \quad M_{xy} \quad Q_x \quad Q_y]^{\mathrm{T}}$$

which is composed of two sub vectors:

$$\boldsymbol{M} = [M_x \quad M_y \quad M_{xy}]^{\mathrm{T}}, \quad \boldsymbol{Q} = [Q_x \quad Q_y]^{\mathrm{T}}$$

Then, the differential equilibrium equations of the thick plate can be written as

$$\left.\begin{aligned} &\frac{\partial M_x}{\partial x} + \frac{\partial M_{xy}}{\partial y} - Q_x - m_x = 0 \\ &\frac{\partial M_{xy}}{\partial x} + \frac{\partial M_y}{\partial y} - Q_y - m_y = 0 \\ &\frac{\partial Q_x}{\partial x} + \frac{\partial Q_y}{\partial y} + q = 0 \end{aligned}\right\} \tag{8-3}$$

One characteristic of the thick plate theory which is different from the thin plate theory is that the number of load densities increases from 1 to 3. Therefore, the shear forces Q_x and Q_y are not only related to the internal moments M_x, M_y and M_{xy}, but also related to the loads m_x and m_y.

8.1.2 Geometrical Equations

The displacements of the thick plate have 3 independent parameters:

$$\boldsymbol{d} = [w \quad \psi_x \quad \psi_y]^{\mathrm{T}} \tag{8-4}$$

in which w is the deflection, and its positive direction is upward; ψ_x is the normal rotation in the xz-plane, and its positive direction is from x-axis to z-axis; ψ_y is the normal rotation in the yz-plane, and its positive direction is from y-axis to z-axis.

The strains of the thick plate have 5 parameters:

$$\boldsymbol{E} = [\kappa_x \quad \kappa_y \quad 2\kappa_{xy} \quad \gamma_x \quad \gamma_y]^{\mathrm{T}} \tag{8-5}$$

where κ_x, κ_y and $2\kappa_{xy}$ are the curvatures, and their positive values are corresponding to the deformations caused by positive M_x, M_y and M_{xy}, respectively. They form a bending strain vector:

$$\boldsymbol{\kappa} = [\kappa_x \quad \kappa_y \quad 2\kappa_{xy}]^{\mathrm{T}} \tag{8-6}$$

γ_x (or γ_{xz}) and γ_y (or γ_{yz}) are shear strains, and their positive values are corresponding to the deformations caused by positive Q_x and Q_y, respectively. They form a shear strain vector:

$$\boldsymbol{\gamma} = [\gamma_x \quad \gamma_y]^{\mathrm{T}} \tag{8-7}$$

The geometrical equations between strains and displacements are as follows:

$$\left.\begin{aligned} &\kappa_x = -\frac{\partial \psi_x}{\partial x}, \quad \kappa_y = -\frac{\partial \psi_y}{\partial y}, \quad 2\kappa_{xy} = -\left(\frac{\partial \psi_x}{\partial y} + \frac{\partial \psi_y}{\partial x}\right) \\ &\gamma_x = \frac{\partial w}{\partial x} - \psi_x, \quad \gamma_y = \frac{\partial w}{\partial y} - \psi_y \end{aligned}\right\} \tag{8-8}$$

After the elimination of w, ψ_x and ψ_y in Eq. (8-8), we obtain

$$\left.\begin{aligned} &\frac{\partial \kappa_x}{\partial y} - \frac{\partial \kappa_{xy}}{\partial x} = \frac{1}{2}\frac{\partial}{\partial x}\left(\frac{\partial \gamma_x}{\partial y} - \frac{\partial \gamma_y}{\partial x}\right) \\ &\frac{\partial \kappa_y}{\partial x} - \frac{\partial \kappa_{xy}}{\partial y} = -\frac{1}{2}\frac{\partial}{\partial y}\left(\frac{\partial \gamma_x}{\partial y} - \frac{\partial \gamma_y}{\partial x}\right) \end{aligned}\right\} \tag{8-9}$$

Then, by the elimination of γ_x and γ_y in Eq. (8-9), we have

$$\frac{\partial^2 \kappa_x}{\partial y^2} + \frac{\partial^2 \kappa_y}{\partial x^2} - 2\frac{\partial^2 \kappa_{xy}}{\partial x \partial y} = 0 \tag{8-10}$$

Equations (8-9) and (8-10) are called the compatibility equations of strains.

Another characteristic of the thick plate theory which is different from the thin plate theory is that the number of displacements increases from 1 to 3. In thin plate, since $\gamma_x = 0$ and $\gamma_y = 0$, from Eq. (8-8), we have

$$\psi_x = \frac{\partial w}{\partial x}, \quad \psi_y = \frac{\partial w}{\partial y}$$

Here, ψ_x and ψ_y can be derived from w, so they are not independent displacement parameters.

8.1.3 Physical Equations

The physical equations between internal forces and strains in a thick plate are as follows:

$$\left.\begin{aligned} M_x &= D(\kappa_x + \mu\kappa_y) \\ M_y &= D(\kappa_y + \mu\kappa_x) \\ M_{xy} &= D(1-\mu)\kappa_{xy} \\ Q_x &= C\gamma_x \\ Q_y &= C\gamma_y \end{aligned}\right\} \tag{8-11}$$

where D and C are the plate bending stiffness and shear stiffness, respectively; μ is the Poisson's ratio. For an isotropic homogenous thick plate, we have

$$D = \frac{Eh^3}{12(1-\mu^2)}, \quad C = \frac{Gh}{k} = \frac{Eh}{2(1+\mu)k} \tag{8-12}$$

where h is the thickness of the plate; E is the Young's modulus; coefficient $k = 1.2$.

For a sandwich plate shown in Fig. 8.2, we have

$$D = \frac{E_f (h+t')^2 t'}{2(1-\mu_f^2)}, \quad C = G_c(h+t') \tag{8-13}$$

where h is the thickness of the core layer; t' is the thickness of the surface layer; E_f and μ_f are the Young's modulus and Poisson's ratio of the surface layer, respectively; G_c is the shear modulus of the core layer.

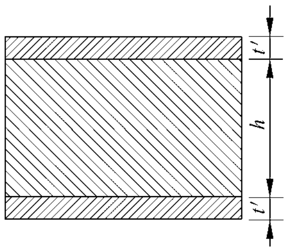

Figure 8.2 A sandwich plate

The physical Eq. (8-11) can be expressed in matrix forms as follows

$$\boldsymbol{M} = \boldsymbol{D}\boldsymbol{\kappa} \tag{8-14}$$

$$\boldsymbol{Q} = \boldsymbol{C}\boldsymbol{\gamma} \tag{8-15}$$

where

$$\boldsymbol{D} = D\begin{bmatrix} 1 & \mu & 0 \\ \mu & 1 & 0 \\ 0 & 0 & \dfrac{1-\mu}{2} \end{bmatrix} \tag{8-16}$$

$$\boldsymbol{C} = C\begin{bmatrix} 1 & 0 \\ 0 & 1 \end{bmatrix} \tag{8-17}$$

Another form of the physical equations is

$$\left.\begin{aligned} \kappa_x &= \frac{M_x - \mu M_y}{D(1-\mu^2)}, \quad \gamma_x = \frac{Q_x}{C} \\ \kappa_y &= \frac{M_y - \mu M_x}{D(1-\mu^2)}, \quad \gamma_y = \frac{Q_y}{C} \\ 2\kappa_{xy} &= \frac{2(1+\mu)M_{xy}}{D(1-\mu^2)} \end{aligned}\right\} \tag{8-18}$$

i.e.,

$$\left.\begin{aligned} \boldsymbol{\kappa} &= \boldsymbol{D}^{-1}\boldsymbol{M} \\ \boldsymbol{\gamma} &= \boldsymbol{C}^{-1}\boldsymbol{Q} \end{aligned}\right\} \tag{8-19}$$

where

$$\boldsymbol{D}^{-1} = \frac{1}{D(1-\mu^2)}\begin{bmatrix} 1 & -\mu & 0 \\ -\mu & 1 & 0 \\ 0 & 0 & 2(1+\mu) \end{bmatrix} \tag{8-20}$$

$$\boldsymbol{C}^{-1} = \frac{1}{C}\begin{bmatrix} 1 & 0 \\ 0 & 1 \end{bmatrix} \tag{8-21}$$

In a thick plate, the shear stiffness C is a finite value, while $C = \infty$ is assumed for the thin plate case.

8.1.4 Coordinate Transformation

Assume that Oxy represents the original coordinate system, $Ox'y'$ represents the new coordinate system, and θ is the rotation from x-axis to x'-axis (see Fig. 8.3).

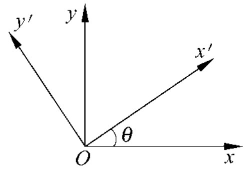

Figure 8.3 Coordinate transformation

Let $l=\cos\theta$, $m=\sin\theta$. Then, the transformation between these two coordinate systems is

$$\begin{Bmatrix} x' \\ y' \end{Bmatrix} = \begin{bmatrix} l & m \\ -m & l \end{bmatrix} \begin{Bmatrix} x \\ y \end{Bmatrix}$$

or written as

$$\boldsymbol{x}' = \boldsymbol{L}\boldsymbol{x} \tag{8-22}$$

where

$$\boldsymbol{L} = \begin{bmatrix} l & m \\ -m & l \end{bmatrix} \tag{8-23}$$

Since

$$\boldsymbol{L}^{-1} = \boldsymbol{L}^{\mathrm{T}}$$

the inverse transformation of Eq. (8-22) is

$$\boldsymbol{x} = \boldsymbol{L}^{\mathrm{T}}\boldsymbol{x}'$$

The transformations of some quantities are the same as Eq. (8-22), for example,

(1) $\dfrac{\partial}{\partial \boldsymbol{x}'} = \boldsymbol{L}\dfrac{\partial}{\partial \boldsymbol{x}}$, i.e., $\begin{Bmatrix} \dfrac{\partial}{\partial x'} \\ \dfrac{\partial}{\partial y'} \end{Bmatrix} = \begin{bmatrix} l & m \\ -m & l \end{bmatrix} \begin{Bmatrix} \dfrac{\partial}{\partial x} \\ \dfrac{\partial}{\partial y} \end{Bmatrix}$

(2) $\boldsymbol{\psi}' = \boldsymbol{L}\boldsymbol{\psi}$, i.e., $\begin{Bmatrix} \psi'_x \\ \psi'_y \end{Bmatrix} = \begin{bmatrix} l & m \\ -m & l \end{bmatrix} \begin{Bmatrix} \psi_x \\ \psi_y \end{Bmatrix}$

(3) $\boldsymbol{\gamma}' = \boldsymbol{L}\boldsymbol{\gamma}$, i.e., $\begin{Bmatrix} \gamma'_x \\ \gamma'_y \end{Bmatrix} = \begin{bmatrix} l & m \\ -m & l \end{bmatrix} \begin{Bmatrix} \gamma_x \\ \gamma_y \end{Bmatrix}$

(4) $\boldsymbol{Q}' = \boldsymbol{L}\boldsymbol{Q}$, i.e., $\begin{Bmatrix} Q'_x \\ Q'_y \end{Bmatrix} = \begin{bmatrix} l & m \\ -m & l \end{bmatrix} \begin{Bmatrix} Q_x \\ Q_y \end{Bmatrix}$ (8-24)

The transformation of moments is similar to the transformation of curvatures:

(1) $\boldsymbol{M}' = \boldsymbol{L}\boldsymbol{M}\boldsymbol{L}^{\mathrm{T}}$, i.e., $\begin{bmatrix} M_{x'} & M_{x'y'} \\ M_{y'x'} & M_{y'} \end{bmatrix} = \begin{bmatrix} l & m \\ -m & l \end{bmatrix} \begin{bmatrix} M_x & M_{xy} \\ M_{yx} & M_y \end{bmatrix} \begin{bmatrix} l & -m \\ m & l \end{bmatrix}$

(2) $\boldsymbol{\kappa}' = \boldsymbol{L}\boldsymbol{\kappa}\boldsymbol{L}^{\mathrm{T}}$, i.e., $\begin{bmatrix} \kappa_{x'} & \kappa_{x'y'} \\ \kappa_{y'x'} & \kappa_{y'} \end{bmatrix} = \begin{bmatrix} l & m \\ -m & l \end{bmatrix} \begin{bmatrix} \kappa_x & \kappa_{xy} \\ \kappa_{yx} & \kappa_y \end{bmatrix} \begin{bmatrix} l & -m \\ m & l \end{bmatrix}$ (8-25)

8.1.5 Boundary Conditions

Assume that n and s stand for the outer normal and tangent directions at an arbitrary point on the boundary, respectively. The angle between n and x-axis is θ (see Fig. 8.4). Let

$$l = \cos\theta, \quad m = \sin\theta$$

from Eqs. (8-24) and (8-25), we obtain

$$\begin{Bmatrix} \dfrac{\partial}{\partial n} \\ \dfrac{\partial}{\partial s} \end{Bmatrix} = \begin{bmatrix} l & m \\ -m & l \end{bmatrix} \begin{Bmatrix} \dfrac{\partial}{\partial x} \\ \dfrac{\partial}{\partial y} \end{Bmatrix} \tag{8-26}$$

$$\begin{Bmatrix} \psi_n \\ \psi_s \end{Bmatrix} = \begin{bmatrix} l & m \\ -m & l \end{bmatrix} \begin{Bmatrix} \psi_x \\ \psi_y \end{Bmatrix} \tag{8-27}$$

$$\left.\begin{aligned} Q_n &= lQ_x + mQ_y \\ M_n &= l^2 M_x + m^2 M_y + 2lmM_{xy} \\ M_{ns} &= (-M_x + M_y)lm + (l^2 - m^2)M_{xy} \end{aligned}\right\} \tag{8-28}$$

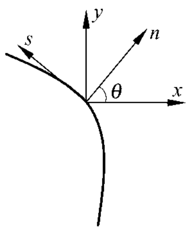

Figure 8.4 The normal and tangent on the boundary

Several typical boundary conditions are given as follows:

$$\left.\begin{array}{ll} w=\bar{w},\quad \psi_n=\bar{\psi}_n,\quad \psi_s=\bar{\psi}_s & \text{(on fixed edge } C_1\text{)} \\ w=\bar{w},\quad \psi_s=\bar{\psi}_s,\quad M_n=\bar{M}_n & \text{(on simply-supported (hard) edge } C_2\text{)} \\ w=\bar{w},\quad M_{ns}=\bar{M}_{ns},\quad M_n=\bar{M}_n & \text{(on simply-supported (soft) edge } C_2'\text{)} \\ M_n=\bar{M}_n,\quad M_{ns}=\bar{M}_{ns},\quad Q_n=\bar{Q}_n & \text{(on free edge } C_3\text{)} \end{array}\right\} \tag{8-29}$$

8.1.6 Strain Energy

Firstly, the definitions of the strain energy density $\tilde{U}$ and the strain energy U of the thick plate are given.

For a given strain vector $\boldsymbol{E}$ (including bending strain $\boldsymbol{\kappa}$ and shear strain $\boldsymbol{\gamma}$):

$$\begin{aligned} \boldsymbol{E} &= [\kappa_x \quad \kappa_y \quad 2\kappa_{xy} \quad \gamma_x \quad \gamma_y]^{\mathrm{T}} \\ \boldsymbol{\kappa} &= [\kappa_x \quad \kappa_y \quad 2\kappa_{xy}]^{\mathrm{T}} \\ \boldsymbol{\gamma} &= [\gamma_x \quad \gamma_y]^{\mathrm{T}} \end{aligned}$$

the function $\tilde{U}(\boldsymbol{E})$ can be defined as

$$\tilde{U}(\boldsymbol{E}) = \tilde{U}_{\mathrm{b}}(\boldsymbol{\kappa}) + \tilde{U}_{\mathrm{s}}(\boldsymbol{\gamma}) \tag{8-30}$$

where

$$\tilde{U}_{\mathrm{b}}(\boldsymbol{\kappa}) = \frac{1}{2}\boldsymbol{\kappa}^{\mathrm{T}}\boldsymbol{D}\boldsymbol{\kappa} = \frac{D}{2}[\kappa_x^2 + \kappa_y^2 + 2\mu\kappa_x\kappa_y + 2(1-\mu)\kappa_{xy}^2] \tag{8-31}$$

$$\tilde{U}_{\mathrm{s}}(\boldsymbol{\gamma}) = \frac{1}{2}\boldsymbol{\gamma}^{\mathrm{T}}\boldsymbol{C}\boldsymbol{\gamma} = \frac{C}{2}(\gamma_x^2 + \gamma_y^2) \tag{8-32}$$

$\tilde{U}(\boldsymbol{E})$ is the strain energy density of the thick plate; $\tilde{U}_{\mathrm{b}}(\boldsymbol{\kappa})$ is the bending strain energy density; $\tilde{U}_{\mathrm{s}}(\boldsymbol{\gamma})$ is the shear strain energy density.

The strain energy U of the thick plate is defined as the functional of the strain fields $\boldsymbol{E}$:

$$\begin{aligned} U(\boldsymbol{E}) &= \iint_{\Omega} \tilde{U}(\boldsymbol{E})\,\mathrm{d}x\mathrm{d}y = \iint_{\Omega}\left(\frac{1}{2}\boldsymbol{\kappa}^{\mathrm{T}}\boldsymbol{D}\boldsymbol{\kappa} + \frac{1}{2}\boldsymbol{\gamma}^{\mathrm{T}}\boldsymbol{C}\boldsymbol{\gamma}\right)\mathrm{d}x\mathrm{d}y \\ &= \iint_{\Omega}\left\{\frac{D}{2}[\kappa_x^2 + \kappa_y^2 + 2\mu\kappa_x\kappa_y + 2(1-\mu)\kappa_{xy}^2] + \frac{C}{2}(\gamma_x^2 + \gamma_y^2)\right\}\mathrm{d}x\mathrm{d}y \end{aligned} \tag{8-33}$$

Two points should be noted:

(1) For arbitrary strain fields $\boldsymbol{E}$, no matter whether these strain fields satisfy the strain compatibility Eq. (8-9), the strain energy corresponding to $\boldsymbol{E}$ can be defined.

If the strain fields $\boldsymbol{E}$ satisfy the strain compatibility Eq. (8-9), and are derived on the basis of the geometrical Eq. (8-8) from certain displacement fields:

$$\boldsymbol{d} = [w \quad \psi_x \quad \psi_y]^{\mathrm{T}}$$

then, the strain energy can be expressed as the functional of the displacement fields,

$$U(\boldsymbol{d}) = \iint_{\Omega} \left\{ \frac{D}{2}\left[\left(\frac{\partial \psi_x}{\partial x} \right)^2 + \left(\frac{\partial \psi_y}{\partial y} \right)^2 + 2\mu \frac{\partial \psi_x}{\partial x}\frac{\partial \psi_y}{\partial y} + \frac{1-\mu}{2}\left(\frac{\partial \psi_x}{\partial y} + \frac{\partial \psi_y}{\partial x} \right)^2 \right] + \frac{C}{2}\left[\left(\frac{\partial w}{\partial x} - \psi_x \right)^2 + \left(\frac{\partial w}{\partial y} - \psi_y \right)^2 \right] \right\} \mathrm{d}x\mathrm{d}y \tag{8-34}$$

(2) From Eqs. (8-31) and (8-32), it can be seen that $\tilde{U}_{\mathrm{b}}(\boldsymbol{\kappa})$ and $\tilde{U}_{\mathrm{s}}(\boldsymbol{\gamma})$ are the positive definite quadric homogeneous functions of (κ_x, κ_y, κ_{xy}) and (γ_x, γ_y), respectively. According to the properties of the positive definite quadric homogeneous function, the following equalities can be obtained:

$$\left.\begin{aligned}
&\frac{\partial \tilde{U}_{\mathrm{b}}}{\partial \kappa_x}\kappa_x + \frac{\partial \tilde{U}_{\mathrm{b}}}{\partial \kappa_y}\kappa_y + \frac{\partial \tilde{U}_{\mathrm{b}}}{\partial \kappa_{xy}}\kappa_{xy} = 2\tilde{U}_{\mathrm{b}} \\
&\frac{\partial \tilde{U}_{\mathrm{s}}}{\partial \gamma_x}\gamma_x + \frac{\partial \tilde{U}_{\mathrm{s}}}{\partial \gamma_y}\gamma_y = 2\tilde{U}_{\mathrm{s}} \\
&\frac{\partial \tilde{U}}{\partial \kappa_x}\kappa_x + \frac{\partial \tilde{U}}{\partial \kappa_y}\kappa_y + \frac{\partial \tilde{U}}{\partial \kappa_{xy}}\kappa_{xy} + \frac{\partial \tilde{U}}{\partial \gamma_x}\gamma_x + \frac{\partial \tilde{U}}{\partial \gamma_y}\gamma_y = 2\tilde{U}
\end{aligned}\right\} \tag{8-35}$$

Secondly, the physical equations between internal forces and strains can be expressed in terms of the strain energy density $\tilde{U}$. For this reason, the derivatives of $\tilde{U}$ are first obtained as follows:

$$\left.\begin{aligned}
&\frac{\partial \tilde{U}}{\partial \kappa_x} = D(\kappa_x + \mu\kappa_y), \quad \frac{\partial \tilde{U}}{\partial \kappa_y} = D(\kappa_y + \mu\kappa_x), \quad \frac{\partial \tilde{U}}{2\partial \kappa_{xy}} = D(1-\mu)\kappa_{xy} \\
&\frac{\partial \tilde{U}}{\partial \gamma_x} = C\gamma_x, \quad \frac{\partial \tilde{U}}{\partial \gamma_y} = C\gamma_y
\end{aligned}\right\} \tag{8-36}$$

From the above equations, it can be seen that the physical Eq. (8-11) can be expressed in terms of the strain energy density $\tilde{U}$ as follows:

$$\left.\begin{aligned}
&M_x = \frac{\partial \tilde{U}}{\partial \kappa_x}, \quad M_y = \frac{\partial \tilde{U}}{\partial \kappa_y}, \quad M_{xy} = \frac{\partial \tilde{U}}{2\partial \kappa_{xy}} \\
&Q_x = \frac{\partial \tilde{U}}{\partial \gamma_x}, \quad Q_y = \frac{\partial \tilde{U}}{\partial \gamma_y}
\end{aligned}\right\} \tag{8-37}$$

Finally, the variation of the strain energy is given as:

$$\delta U = \iint_{\Omega} \delta \tilde{U} \mathrm{d}x\mathrm{d}y \tag{8-38}$$

i.e.,

$$\begin{aligned}\delta U &= \iint_{\Omega} \left[\frac{\partial \tilde{U}}{\partial \kappa_x} \delta \kappa_x + \frac{\partial \tilde{U}}{\partial \kappa_y} \delta \kappa_y + \frac{\partial \tilde{U}}{\partial \kappa_{xy}} \delta \kappa_{xy} + \frac{\partial \tilde{U}}{\partial \gamma_x} \delta \gamma_x + \frac{\partial \tilde{U}}{\partial \gamma_y} \delta \gamma_y \right] \mathrm{d}x\mathrm{d}y \\ &= \iint_{\Omega} [M_x \delta \kappa_x + M_y \delta \kappa_y + 2M_{xy} \delta \kappa_{xy} + Q_x \delta \gamma_x + Q_y \delta \gamma_y] \mathrm{d}x\mathrm{d}y\end{aligned} \tag{8-39}$$

The above equation indicates that the variation of the strain energy equals to the work done by the corresponding internal forces on the variation of strains.

8.1.7 Strain Complementary Energy

Firstly, the definitions of the strain complementary energy density $\tilde{V}$ and strain complementary energy V of the thick plate are given.

For a given internal force vector $\boldsymbol{S}$ (including internal moments $\boldsymbol{M}$ and shear forces $\boldsymbol{Q}$):

$$\left.\begin{aligned} \boldsymbol{S} &= [M_x \quad M_y \quad M_{xy} \quad Q_x \quad Q_y]^{\mathrm{T}} \\ \boldsymbol{M} &= [M_x \quad M_y \quad M_{xy}]^{\mathrm{T}} \\ \boldsymbol{Q} &= [Q_x \quad Q_y]^{\mathrm{T}} \end{aligned}\right\} \tag{8-40}$$

the function $\tilde{V}(\boldsymbol{S})$ can be defined as:

$$\tilde{V}(\boldsymbol{S}) = \tilde{V}_{\mathrm{b}}(\boldsymbol{M}) + \tilde{V}_{\mathrm{s}}(\boldsymbol{Q}) \tag{8-41}$$

$$\tilde{V}_{\mathrm{b}}(\boldsymbol{M}) = \frac{1}{2} \boldsymbol{M}^{\mathrm{T}} \boldsymbol{D}^{-1} \boldsymbol{M} = \frac{1}{2(1-\mu^2)D} [M_x^2 + M_y^2 - 2\mu M_x M_y + 2(1+\mu) M_{xy}^2] \tag{8-42}$$

$$\tilde{V}_{\mathrm{s}}(\boldsymbol{Q}) = \frac{1}{2} \boldsymbol{Q}^{\mathrm{T}} \boldsymbol{C}^{-1} \boldsymbol{Q} = \frac{1}{2C} (Q_x^2 + Q_y^2) \tag{8-43}$$

$\tilde{V}(\boldsymbol{S})$ is the strain complementary energy density of the thick plate; $\tilde{V}_{\mathrm{b}}(\boldsymbol{M})$ is the bending strain complementary energy density; $\tilde{V}_{\mathrm{s}}(\boldsymbol{Q})$ is the shear strain complementary energy density.

The strain complementary energy V of the thick plate is defined as the functional of the internal force fields $\boldsymbol{S}$:

$$V(\boldsymbol{S})=\iint_{\Omega}\tilde{V}(\boldsymbol{S})\mathrm{d}x\mathrm{d}y=\iint_{\Omega}\left(\frac{1}{2}\boldsymbol{M}^{\mathrm{T}}\boldsymbol{D}^{-1}\boldsymbol{M}+\frac{1}{2}\boldsymbol{Q}^{\mathrm{T}}\boldsymbol{C}^{-1}\boldsymbol{Q}\right)\mathrm{d}x\mathrm{d}y$$
$$=\iint_{\Omega}\left\{\frac{1}{2(1-\mu^2)D}[M_x^2+M_y^2-2\mu M_x M_y+2(1+\mu)M_{xy}^2]+\frac{1}{2C}(Q_x^2+Q_y^2)\right\}\mathrm{d}x\mathrm{d}y \tag{8-44}$$

Two points should be noted:

(1) For arbitrary internal force fields $\boldsymbol{S}$, no matter whether these internal force fields satisfy the equilibrium differential Eq. (8-3) and boundary conditions under given loads, the strain complementary energy corresponding to $\boldsymbol{S}$ can be defined.

(2) From Eqs. (8-42) and (8-43), it can be seen that $\tilde{V}_{\mathrm{b}}(\boldsymbol{M})$ and $\tilde{V}_{\mathrm{s}}(\boldsymbol{Q})$ are the positive definite quadric homogeneous functions of (M_x, M_y, M_{xy}) and (Q_x, Q_y), respectively. According to the properties of the positive definite quadric homogeneous function, the following equalities can be obtained:

$$\left.\begin{aligned}
&\frac{\partial\tilde{V}_{\mathrm{b}}}{\partial M_x}M_x+\frac{\partial\tilde{V}_{\mathrm{b}}}{\partial M_y}M_y+\frac{\partial\tilde{V}_{\mathrm{b}}}{\partial M_{xy}}M_{xy}=2\tilde{V}_{\mathrm{b}}\\
&\frac{\partial\tilde{V}_{\mathrm{s}}}{\partial Q_x}Q_x+\frac{\partial\tilde{V}_{\mathrm{s}}}{\partial Q_y}Q_y=2\tilde{V}_{\mathrm{s}}\\
&\frac{\partial\tilde{V}}{\partial M_x}M_x+\frac{\partial\tilde{V}}{\partial M_y}M_y+\frac{\partial\tilde{V}}{\partial M_{xy}}M_{xy}+\frac{\partial\tilde{V}}{\partial Q_x}Q_x+\frac{\partial\tilde{V}}{\partial Q_y}Q_y=2\tilde{V}
\end{aligned}\right\} \tag{8-45}$$

The derivatives of the strain complementary energy density are given as follows:

$$\left.\begin{aligned}
&\frac{\partial\tilde{V}}{\partial M_x}=\frac{M_x-\mu M_y}{D(1-\mu^2)},\quad \frac{\partial\tilde{V}}{\partial Q_x}=\frac{Q_x}{C}\\
&\frac{\partial\tilde{V}}{\partial M_y}=\frac{M_y-\mu M_x}{D(1-\mu^2)},\quad \frac{\partial\tilde{V}}{\partial Q_y}=\frac{Q_y}{C}\\
&\frac{\partial\tilde{V}}{\partial M_{xy}}=\frac{2(1+\mu)}{D(1-\mu^2)}M_{xy}
\end{aligned}\right\} \tag{8-46}$$

By using the above derivative formulae, the physical Eq. (8-18) between internal forces and strains can be expressed in terms of the strain complementary energy density $\tilde{V}$ as follows:

$$\left.\begin{aligned}
&\kappa_x=\frac{\partial\tilde{V}}{\partial M_x},\quad \gamma_x=\frac{\partial\tilde{V}}{\partial Q_x}\\
&\kappa_y=\frac{\partial\tilde{V}}{\partial M_y},\quad \gamma_y=\frac{\partial\tilde{V}}{\partial Q_y}\\
&2\kappa_{xy}=\frac{\partial\tilde{V}}{\partial M_{xy}}
\end{aligned}\right\} \tag{8-47}$$

Finally, the variation of the strain complementary energy is given as:

$$\delta V = \iint_{\Omega} \delta \tilde{V} \mathrm{d}x\mathrm{d}y$$
$$= \iint_{\Omega} \left[\frac{\partial \tilde{V}}{\partial M_x} \delta M_x + \frac{\partial \tilde{V}}{\partial M_y} \delta M_y + \frac{\partial \tilde{V}}{\partial M_{xy}} \delta M_{xy} + \frac{\partial \tilde{V}}{\partial Q_x} \delta Q_x + \frac{\partial \tilde{V}}{\partial Q_y} \delta Q_y \right] \mathrm{d}x\mathrm{d}y \tag{8-48}$$

Substitution of Eq. (8-47) into the above equation yields

$$\delta V = \iint_{\Omega} [\kappa_x \delta M_x + \kappa_y \delta M_y + 2\kappa_{xy} \delta M_{xy} + \gamma_x \delta Q_x + \gamma_y \delta Q_y] \mathrm{d}x\mathrm{d}y$$

The above equation indicates that the variation of the strain complementary energy equals to the work done by the variation of internal forces on the corresponding strains.

8.2 Comparison of the Theories for Thick Plates and Thin Plates

According to the contents in the previous section, this section will introduce the differences between the theories for thick plates and thin plates. Comparisons are made in fundamental equations and typical numerical examples.

8.2.1 Comparison of Fundamental Equations

1. Notes on the basic assumptions of deformation

In the thin plate theory, the Kirchhoff normal assumption is adopted—The normal of the mid-surface before deformation will still be the normal of the mid-surface after deformation.

In the thick plate theory, the Reissner-Mindlin straight-line assumption is adopted—The normal of the mid-surface before deformation will still be a straight line after deformation, but generally not the normal of the mid-surface anymore.

One uses the normal assumption while the other uses the straight-line assumption, this exhibits the essential difference of the two theories.

2. Notes on the shear deformation problem

Since the Kirchhoff normal assumption is adopted in the thin plate theory, the transverse shear strains γ_x and γ_y will keep zero during the deformations of the thin plates, and then, the normal rotations ψ_x and ψ_y will keep being equal to the mid-surface slopes $\frac{\partial w}{\partial x}$ and $\frac{\partial w}{\partial y}$, as shown in Eq. (8-2).

The Reissner-Mindlin straight-line assumption is adopted in the thick plate theory, hence, in general, the normal rotations ψ_x and ψ_y of the thick plates will not keep being equal to the mid-surface slopes $\frac{\partial w}{\partial x}$ and $\frac{\partial w}{\partial y}$. Their differences are the transverse shear strains γ_x and γ_y, as shown in Eq. (8-1).

The essential differences between these two plate theories are:

(1) Whether the influences of the transverse shear strains are considered or not.

(2) Whether the normal rotations are equal to the mid-surface slopes or not.

From above, we can also conclude that:

(1) For shear stiffness: $C=\infty$ is assumed in the thin plate theory while C is a finite value in the thick plate theory.

(2) For strain energy: in the thick plate theory, strain energy U is the sum of the bending strain energy U_b and the shear strain energy U_s; while in the thin plate theory, $U=U_b$ because of $U_s=0$.

That the shear stiffness C is looked upon as infinite, and the shear strain energy U_s is neglected, are the inevitable results of ignoring the influences of shear deformations in the thin plate theory.

3. Notes on the independent displacements in w, ψ_x and ψ_y

In the thin plate theory, ψ_x and ψ_y are equal to the derivatives of w, so they are not independent displacements. Thus, in the 3 displacements w, ψ_x and ψ_y, only w is independent.

In the thick plate theory, since two new fields γ_x and γ_y appear, w, ψ_x and ψ_y are 3 independent displacement fields.

Independence or dependence between the displacement fields w and (ψ_x, ψ_y) is another essential difference between these two plate theories.

When constructing a universal displacement-based element for both thick and thin plates, one main difficulty encountered is how to deal with the dual requirements of independence and dependence.

Only one independent displacement w is considered for constructing the thin plate element, while 3 independent displacements w, ψ_x and ψ_y must be taken into account for constructing the thick plate element. From this viewpoint, it seems that the development of a thick plate element is more complicated than that of a thin plate element. But, if we observe the expressions of strain energy, it can be seen that the integrands in the strain energy expression (8-34) of the thick plate element contain only first-order derivatives of w, ψ_x and ψ_y, so it belongs to C^0-continuity problem. On the other hand, the integrands in the strain energy expression of the thin plate element contain second-order derivatives of w, thus, it belongs to C^1-continuity problem. Therefore, the construction of the thick plate elements is indeed easier than that of the thin plate element. Anyway, it is easier to construct elements special for the thick plates, but more difficult to construct elements special for the thin plates, and much more difficult to develop universal elements for both thick and thin plates.

4. Notes on the boundary conditions

In the thick plate theory, several typical boundary conditions have been given by Eq. (8-29), in which each boundary has 3 boundary conditions, i.e.,

On fixed edge C_1

$$w=\bar{w},\quad \psi_s=\bar{\psi}_s,\quad \psi_n=\bar{\psi}_n \tag{8-49a,b,c}$$

On simply-supported (hard) edge C_2

$$w=\bar{w},\quad \psi_s=\bar{\psi}_s,\quad M_n=\bar{M}_n \tag{8-50a,b,c}$$

On simply-supported (soft) edge C_2'

$$w=\bar{w},\quad M_{ns}=\bar{M}_{ns},\quad M_n=\bar{M}_n \tag{8-51a,b,c}$$

On free edge C_3

$$M_n=\bar{M}_n,\quad M_{ns}=\bar{M}_{ns},\quad Q_n=\bar{Q}_n \tag{8-52a,b,c}$$

Here, the conditions on the fixed edge are all displacement conditions; conditions on the free edge are all force conditions; and conditions on the simply-supported edge are mixed conditions of displacement and force.

In the thin plate theory, since the transverse shear strains are assumed to be zero, the following assumption

$$\psi_s=\frac{\partial w}{\partial s} \tag{8-53}$$

is imposed on the boundary. Thus, the boundary tangent rotation ψ_s is a non-independent displacement relied on boundary deflection w, thereupon, the number of DOFs at each point of the boundary will decrease from 3 (w, ψ_s, ψ_n) to 2 (w, ψ_n), and the number of the boundary conditions will also decrease from 3 to 2.

Firstly, let us consider the fixed edge case. According to the assumption given in Eq. (8-53), the second boundary condition in Eq. (8-49) can be derived from the first boundary condition. So, after the elimination of this non-independent condition, only 2 independent boundary conditions (8-49a,c) remain.

Secondly, let us consider the simply-supported edge case. In the thin plate theory, there are 2 boundary conditions on the simply-supported edge:

$$w=\bar{w},\quad M_n=\bar{M}_n$$

These are Eqs. (8-50a,c), and also Eqs. (8-51a,c). In the thick plate theory, there are 3 boundary conditions on the simply-supported edge, that is to say, one condition of tangent rotation along the boundary should be supplemented. If the displacement condition (8-50b) $\psi_s = \overline{\psi}_s$ is supplemented, then the boundary is called as hard simply-supported edge; if the force condition (8-51b) $M_{ns} = \overline{M}_{ns}$ is supplemented, then the boundary is called as soft simply-supported edge. Therefore, in the thick plate theory, there are two types of simply-supported edge: hard and soft; but in the thin plate theory, only one type exists.

Finally, let us consider the free edge case. In the thin plate theory, the boundary conditions (8-52) will be replaced by the following two conditions:

On free edge C_3

$$M_n = \overline{M}_n, \quad \frac{\partial M_{ns}}{\partial s} + Q_n = \overline{V}_n \tag{8-54a,b}$$

i.e., two conditions (b) and (c) in Eq. (8-52) are replaced by one condition (b) in Eq. (8-54). Indeed, this is also the inevitable result by introducing the assumption (8-53). Here, $\overline{V}_n$ is the density of the distributed transverse load along the free edge of the thin plate.

Now, from the viewpoint of virtual work, the boundary conditions on the free edge in thick and thin plate theories are explained as follows.

In the thick plate theory, there are 3 independent displacements w, ψ_n and ψ_s on the free boundary edge. Assume that the virtual displacements on the free edge are δw, $\delta\psi_n$ and $\delta\psi_s$, the virtual work done by the boundary forces is

$$\delta W = \int_{C_3} [-M_n \delta\psi_n - M_{ns}\delta\psi_s + Q_n \delta w]\mathrm{d}s \tag{8-55}$$

On the other hand, the virtual work done by the given loads on the free edge is

$$\delta \overline{W} = \int_{C_3} [-\overline{M}_n \delta\psi_n - \overline{M}_{ns}\delta\psi_s + \overline{Q}_n \delta w]\mathrm{d}s \tag{8-56}$$

Let $\delta W = \delta\overline{W}$, and since the virtual displacements δw, $\delta\psi_n$ and $\delta\psi_s$ are 3 independent arbitrary functions, the 3 boundary conditions in Eqs. (8-52a,b,c) can be obtained.

In the thin plate theory, since the assumption in Eq. (8-53) is introduced, there are only 2 independent virtual displacements δw and $\delta\psi_n$, and $\delta\psi_s = \frac{\partial \delta w}{\partial s}$. The work done by the boundary force is

$$\delta W = \int_{C_3} \left[-M_n \delta\psi_n - M_{ns}\frac{\partial \delta w}{\partial s} + Q_n \delta w \right]\mathrm{d}s \tag{8-57}$$

By using the formula of integration by parts, we obtain

$$\delta W = \int_{C_3} \left[-M_n \delta \psi_n + \left(\frac{\partial M_{ns}}{\partial s} + Q_n \right) \delta w \right] \mathrm{d}s - M_{ns}\, \delta w \Big|_{C_3^-}^{C_3^+} \tag{8-58}$$

in which C_3^- and C_3^+ are two ends of the free edge. Since the two ends of the free edge link with the fixed edge or the simply-supported edge, at C_3^- and C_3^+, $\delta w = 0$, and then the above equation can be written as

$$\delta W = \int_{C_3} \left[-M_n \delta \psi_n + \left(\frac{\partial M_{ns}}{\partial s} + Q_n \right) \delta w \right] \mathrm{d}s \tag{8-59}$$

On the other hand, the work done by the given loads on the free edge is

$$\delta \overline{W} = \int_{C_3} [- \overline{M}_n \delta \psi_n + \overline{V}_n \delta w] \mathrm{d}s \tag{8-60}$$

Let $\delta W = \delta \overline{W}$, and since $\delta \psi_n$ and δw are 2 arbitrary functions, the 2 boundary conditions on the free edge of the thin plate can be obtained, as shown in Eq. (8-54a,b).

The above discussions about the boundary conditions are expounded from the viewpoint of virtual work. This expatiation method is very natural and evident.

In the thick plate theory, the expression of the boundary virtual work is Eq. (8-55), where ψ_n, ψ_s and w are 3 independent generalized displacements; and $(-M_n)$, $(-M_{ns})$ and Q_n are 3 conjugate (or corresponding) independent generalized forces, respectively. Thereby, in the thick plate theory, there are 3 independent boundary conditions, which are generally expressed by

$$\psi_n = \overline{\psi}_n \quad \text{or} \quad M_n = \overline{M}_n \tag{8-61a}$$

$$\psi_s = \overline{\psi}_s \quad \text{or} \quad M_{ns} = \overline{M}_{ns} \tag{8-61b}$$

$$w = \overline{w} \quad \text{or} \quad Q_n = \overline{Q}_n \tag{8-61c}$$

In the thin plate theory, the expression of boundary virtual work is Eq. (8-59), where ψ_n and w are 2 independent generalized displacements; and $(-M_n)$ and $\left(\frac{\partial M_{ns}}{\partial s} + Q_n \right)$ are 2 conjugate (or corresponding) independent generalized forces, respectively. Thereby, in the thin plate theory, there are 2 independent boundary conditions, which are generally expressed by

$$\psi_n = \overline{\psi}_n \quad \text{or} \quad M_n = \overline{M}_n \tag{8-62a}$$

$$w = \bar{w} \quad \text{or} \quad \frac{\partial M_{ns}}{\partial s} + Q_n = \bar{V}_n \tag{8-62b}$$

where $\frac{\partial M_{ns}}{\partial s}$ is called as the equivalent transverse shear force of the twisting moment M_{ns}; and $\frac{\partial M_{ns}}{\partial s} + Q_n = V_n$ is called as the resultant transverse shear force.

In the above discussions, the concept that the generalized force P and the generalized displacement $\varDelta$ are conjugate with each other is mentioned. Its definition can be given as follows.

If the virtual work W done by the generalized force P along the generalized displacement $\varDelta$ is equal to the product $P\varDelta$, i.e.,

$$W = P\varDelta \tag{8-63}$$

then, we say that the generalized displacement $\varDelta$ and the generalized force P are conjugate with each other (or corresponding to each other).

5. Notes on the independent load components and internal force components

Firstly, let us discuss the load components.

In the thick plate theory, since there are 3 independent displacement components w, ψ_x and ψ_y, there should be 3 independent load components q, m_x and m_y corresponding to them. So, the expression of virtual work is

$$\delta W = \iint_A [q\delta w + m_x \delta \psi_x + m_y \delta \psi_y] \mathrm{d}A \tag{8-64}$$

From this virtual work expression, it can be seen that 3 load components and 3 displacement components are corresponding to or conjugate with each other.

In the thin plate theory, since there is only one independent transverse displacement component w, and the rotation components ψ_x and ψ_y are both relied on w, there should be only one independent transverse load component q corresponding to it, and the couple load components m_x and m_y should be converted to equivalent transverse load components on dA with line distributed transverse load on the boundary ds. So, the expression of virtual work is

$$\begin{aligned}\delta W &= \iint_A \left[q\delta w + m_x \frac{\partial \delta w}{\partial x} + m_y \frac{\partial \delta w}{\partial y} \right] \mathrm{d}A \\ &= \iint_A \left(q - \frac{\partial m_x}{\partial x} - \frac{\partial m_y}{\partial y} \right) \delta w \mathrm{d}A + \oint_{\partial A} (m_x l + m_y m) \delta w \mathrm{d}s\end{aligned} \tag{8-65}$$

Therefore, after conversion, the surface load q^* and boundary load V_n^* are

$$q^* = q - \frac{\partial m_x}{\partial x} - \frac{\partial m_y}{\partial y} \tag{8-66a}$$

$$V_n^* = m_x l + m_y m \tag{8-66b}$$

Secondly, let us discuss the internal force components.

In the thick plate theory, there are 5 independent internal force components. That is to say, besides the bending moments M_x, M_y and twisting moment M_{xy}, the transverse shear forces Q_x and Q_y are also independent internal force components. It can be seen from the equilibrium differential Eq. (8-3) that, since there are independent couple load components m_x and m_y existing, Q_x and Q_y in the thick plate theory do not completely rely on M_x, M_y and M_{xy}, they are independent internal force components. On the contrary, in the thin plate theory, since $m_x = m_y = 0$ is assumed, Q_x and Q_y completely rely on M_x, M_y and M_{xy}, Q_x and Q_y will not be looked upon as independent internal force components. That is to say, there are only 3 independent internal force components in the thin plate theory.

8.2.2 Comparison of Typical Examples

1. The special case in which the same internal force solution is obtained by both thin beam theory and thick beam theory in beam and frame analysis

The beam theories can be classified as thin beam theory and thick beam theory. Their difference is whether the influence of the shear strain is ignored or not.

When these two theories are employed in beam and frame analysis, except the special case of pure bending state in which the shear strain is zero, the displacement solutions of the two theories are generally different, but the internal force solutions may be either same or different. Now, we discuss the case in which the internal force solutions are the same as each other.

Firstly, if beam and frame are statically determinate structures, the internal force solutions by the two theories will be the same as each other, but for displacement solutions, there will be a discrepancy of an additional displacement purely caused by shear strain, i.e.,

$$M = M^0, \quad Q = Q^0 \tag{8-67}$$

$$\varDelta = \varDelta^0 + \tilde{\varDelta}(\gamma) \tag{8-68}$$

where M, Q and $\varDelta$ are the bending moment, shear force and displacement of the thick beam theory, respectively; M^0, Q^0 and $\varDelta^0$ are the bending moment, shear force and displacement of the thin beam theory, respectively; $\tilde{\Delta}(\gamma)$ is the additional displacement caused by shear strain.

Secondly, consider the case of the statically indeterminate structures. If the following examples are considered:

(1) the shear force is statically determinate (Fig. 8.5(a));

(2) the shear force is statically determinate under symmetrical load (Fig. 8.6(a));

(3) the shear force of the non-rigid bar is statically determinate (Fig. 8.7(a), there is still a rigid bar in the frame, but its shear strain is identically equal to zero, so it is not necessary to consider whether its shear forces are statically determinate).

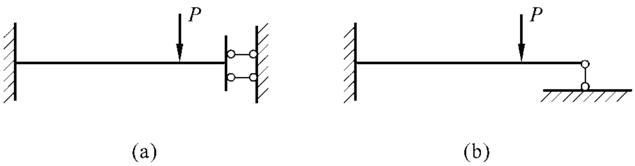

Figure 8.5 Statically indeterminate beams

(a) A slipping support at the right end; (b) A vertical support at the right end

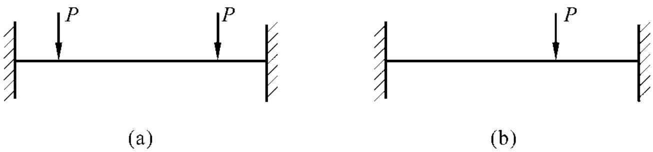

Figure 8.6 Statically indeterminate symmetrical beams

(a) Symmetrical load; (b) Unsymmetrical load

It follows that the internal force solutions by the two theories will be the same as each other.

For comparison, examples which do not belong to the above cases are given in Figs. 8.5(b), 8.6(b) and 8.7(b).

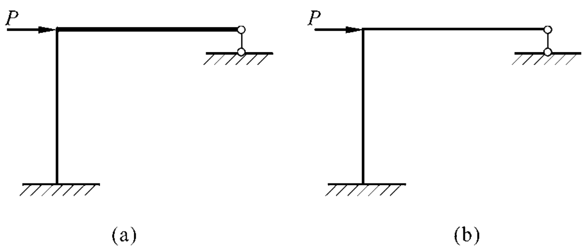

Figure 8.7 Statically indeterminate frames

(a) Horizontal beam is a rigid bar; (b) Horizontal beam is not a rigid bar

The above conclusion can be proved as follows.

Assume that the degree of statical indeterminacy for the structure is n. The structure is analyzed using the force method, and the corresponding statically determinate structure is taken as the basic structure. In the n redundant unknown forces, assume that m forces are nonzero ($m \leqslant n$), then the bending moment M and shear force Q can be expressed as

$$M = M_P + \sum_{i=1}^{m} \bar{M}_i X_i \tag{8-69a}$$

$$Q = Q_P + \sum_{i=1}^{m} \bar{Q}_i X_i \tag{8-69b}$$

where M_P and Q_P are the internal forces caused by loads in the basic structure; $\bar{M}_i$ and $\bar{Q}_i$ are the internal forces caused by unit redundant force $X_i = 1$ in the basic structure; $X_1, X_2, \cdots, X_m$ are m nonzero redundant unknown forces. M_P, $\bar{M}_i$, Q_P, $\bar{Q}_i$ are all determined by the equilibrium conditions.

Since the shear forces of each non-rigid bar are assumed to be statically determinate, for each non-rigid bar, we can set

$$\bar{Q}_i = 0 \quad (i = 1, 2, \cdots, m) \tag{8-70}$$

The redundant unknown forces $X_1, X_2, \cdots, X_m$ can be solved by the fundamental equations of force method.

For the thick beam theory, we have

$$\sum_{j=1}^{m} \delta_{ij} X_i + \varDelta_{iP} = 0 \quad (i = 1, 2, \cdots, m)$$

where

$$\delta_{ij} = \sum \int \frac{\bar{M}_i \bar{M}_j}{D} \mathrm{d}s + \sum \int \frac{\bar{Q}_i \bar{Q}_j}{C} \mathrm{d}s$$

$$\varDelta_{iP} = \sum \int \frac{\bar{M}_i M_P}{D} \mathrm{d}s + \sum \int \frac{\bar{Q}_i Q_P}{C} \mathrm{d}s$$

in which D and C are the section bending and shearing stiffness, respectively.

For the thin beam theory, we have

$$\sum_{j=1}^{m} \delta_{ij}^0 X_i + \varDelta_{iP}^0 = 0 \quad (i = 1, 2, \cdots, m)$$

where

$$\delta_{ij}^0 = \sum \int \frac{\bar{M}_i \bar{M}_j}{D} \mathrm{d}s$$

$$\varDelta_{iP}^0 = \sum \int \frac{\bar{M}_i M_P}{D} \mathrm{d}s$$

By using Eq. (8-70), we have

$$\delta_{ij} = \delta_{ij}^0, \quad \Delta_{iP} = \Delta_{iP}^0 \tag{8-71}$$

Therefore, the redundant unknown forces $X_1, X_2, \cdots, X_m$ solved by the two theories are the same as each other. Substituting these solutions into Eq. (8-69), it can be seen that the internal force solutions obtained by the two theories are the same as each other. □

2. The special case in which the same internal force solution is obtained by both thin plate theory and thick plate theory

The following problems belong to this special case:

(1) Simply-supported polygonal plate;

(2) Circular plate with axisymmetric deformation;

(3) The plate problems in which the shear forces Q_x and Q_y are statically determinate.

The proofs about the above conclusions can be referred to reference [3].

3. The concentrated load problem

Consider a clamped circular plate (the radius is a) subjected to a concentrated load P at the center point C.

The displacement solution and the deflection at point C of the thin plate theory are

$$w^0 = \frac{Pr^2}{8\pi D}\ln\frac{r}{a} + \frac{P}{16\pi D}(a^2 - r^2) \tag{8-72a}$$

$$w_C^0 = \frac{Pa^2}{16\pi D} \tag{8-72b}$$

The displacement solutions and the deflection at point C of the thick plate theory are

$$w = w^0 - \frac{P}{2\pi C}\ln\frac{r}{a} \tag{8-73a}$$

$$\psi_r = \frac{\mathrm{d}w^0}{\mathrm{d}r} \tag{8-73b}$$

$$w_C = \infty \tag{8-73c}$$

From the above results, it can be seen that, the deflection at the load point C of the concentrated load is a finite value by the thin plate theory, but an infinite value by the thick plate theory. This distinction is completely caused by the influence of the shear strain. In fact, the second term at the right side of Eq. (8-73a) is the additional deflection $\tilde{w}(r)$ purely caused by shear strain.

$$\tilde{w}(r) = -\frac{P}{2\pi C}\ln\frac{r}{a} \tag{8-74}$$

The above equation can be derived as follows.

Firstly, the shear force Q_r is statically determinate, i.e.,

$$Q_r = -\frac{P}{2\pi r} \tag{8-75}$$

The shear strain γ_r is

$$\gamma_r = \frac{Q_r}{C} = -\frac{P}{2\pi rC} \tag{8-76}$$

Secondly, $\tilde{\psi}_r = 0$ should be assumed when the additional deflection $\tilde{w}$ caused by the shear strain is being solved, so we obtain

$$\frac{\mathrm{d}\tilde{w}}{\mathrm{d}r} = \gamma_r = -\frac{P}{2\pi rC}$$

After integration, we have

$$\tilde{w} = -\frac{P}{2\pi C}\ln r + C_1$$

where constant C_1 can be solved by the boundary condition $w\big|_{r=a} = 0$ at $r = a$. Finally, Eq. (8-74) can be obtained. □

From Eqs. (8-75) and (8-76), it can be seen that the values of Q_r and γ_r at point C are both infinite, which are corresponding to the result $\tilde{w}_C = \infty$.

4. High-order vibration problem

In the vibration analysis of plate, there are two different points between the thick and thin plate theories: one is whether the influence of shear deformation is considered; the other is whether the influence of rotary inertia is considered.

In order to explain the distinction of the second point, the kinetic equations for the natural vibration problem of the thick plate are given as follows:

$$\frac{\partial M_x}{\partial x} + \frac{\partial M_{xy}}{\partial y} - Q_x - \omega^2 \rho J \psi_x = 0 \tag{8-77a}$$

$$\frac{\partial M_{xy}}{\partial x}+\frac{\partial M_{y}}{\partial y}-Q_{y}-\omega^{2}\rho J\psi_{y}=0 \tag{8-77b}$$

$$\frac{\partial Q_{x}}{\partial x}+\frac{\partial Q_{y}}{\partial y}+\omega^{2}\rho h w=0 \tag{8-77c}$$

where ω is the natural frequency; ρ is the density of material; ρh is the mass of the unit area on the mid-surface of the plate; ρJ is the rotary inertia. In the thin plate theory, the influence of rotary inertia is ignored.

In high-order vibrations, the effective length and width of the high-order modes become smaller, so the influence of rotary inertia and shear deformation will increase. Thereby, although a plate may belong to the thin plate type, for the analysis of the high-order vibration of this thin plate, it is more reasonable to employ the thick plate theory.

5. Stress concentration problem near a circular hole

Consider an infinite plate with a circular hole (the radius is a). At its infinite edge, the plate is under pure bending state along x-axis, i.e., $M_x=M_0$, and other internal force components are all zero. Now, let us solve the stress concentration coefficient k_B near the circular hole, which is defined as

$$k_B=\frac{M_{\theta\max}}{M_0} \tag{8-78}$$

where $M_{\theta\max}$ denotes the maximum value of the bending moment M_θ at the circular hole boundary.

According to the thin plate theory, we have

$$k_B^0=\frac{5+3\mu}{3+\mu} \tag{8-79}$$

When the Poisson's ratio $\mu=\frac{1}{3}$, $k_B^0=1.8$.

According to the Reissner thick plate theory, we have

$$k_B=\frac{3}{2}+\frac{1}{2}\cdot\frac{\frac{3}{2}(1+\mu)K_2\left(\sqrt{10}\frac{a}{h}\right)-K_0\left(\sqrt{10}\frac{a}{h}\right)}{\frac{1}{2}(1+\mu)K_2\left(\sqrt{10}\frac{a}{h}\right)+K_0\left(\sqrt{10}\frac{a}{h}\right)} \tag{8-80}$$

where K_0 and K_2 are the modified Bessel functions. When $\mu=\frac{1}{3}$, the variations of k_B and k_B^0 are plotted in Fig. 8.8 and listed in Table 8.1.

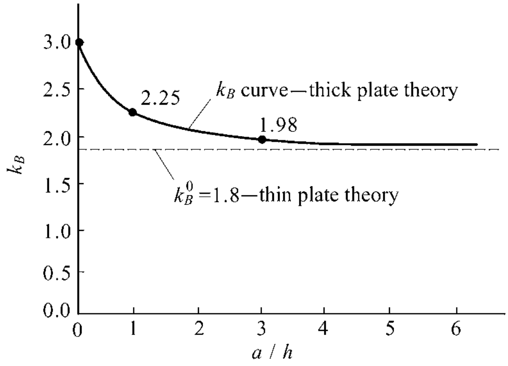

Figure 8.8 The stress concentration coefficient (μ= 1/3)

Table 8.1 The comparison between stress concentration coefficients k_B and k_B^0

a/h	0	1	3
Solution of thick plate theory k_B	3.00	2.25	1.98
Solution of thin plate theory k_B^0	1.80	1.80	1.80
Error $\frac{k_B - k_B^0}{k_B}$	40%	20%	9%

It can be seen that, in the stress concentration problems of plate bending, the influence of the transverse shear strain should not be ignored. The solution of the thin plate theory k_B^0 is always less than the solution of the thick plate theory k_B. Therefore, the solution of the thin plate theory is more unsafe. Errors will increase with the decrease of *a/h*, and the maximum error is up to 40%.

6. Stress distribution near free edge

As pointed out in the previous sections, for the boundary conditions of the free edge, the expressions from the two theories are different: the thick plate theory requires 3 boundary conditions (8-52a,b,c) to be satisfied, but thin plate theory cannot satisfy them and requires only 2 boundary conditions (8-54a,b) to be satisfied. Therefore, the solutions on or near the free edge of the two theories are always discrepant.

In order to understand the discrepancy in the solutions near the free edge of the two theories, the stress concentration problem near a circular hole mentioned above is still used to illustrate the problem of this section.

Firstly, according to thin plate theory, solutions of Q_r^0 , $M_{r\theta}^0$ and V_r are

$$\left.\begin{aligned} Q_r^0 &= \frac{4}{3+\mu} M_0 \frac{a^2}{r^3} \cos 2\theta \\ M_{r\theta}^0 &= \frac{1}{3+\mu} M_0 \left[-2 + (1-\mu)\left(\frac{a^2}{r^2} - 1\right) - \frac{3}{2}(1-\mu)\left(\frac{a^4}{r^4} - 1\right) \right] \sin 2\theta \\ V_r &= \frac{1}{3+\mu} M_0 \frac{1}{r} \left[2(3-\mu)\left(\frac{a^2}{r^2} - 1\right) - 3(1-\mu)\left(\frac{a^4}{r^4} - 1\right) \right] \cos 2\theta \end{aligned}\right\} \quad (8\text{-}81)$$

It can be seen that at the boundary $r = a$ of the circular hole, only the boundary condition $V_r = 0$ is satisfied, while Q_r^0 and $M_{r\theta}^0$ are both nonzero at the boundary.

Secondly, according to the thick plate theory, the solutions of Q_r and $M_{r\theta}$ are

$$\left.\begin{aligned} Q_r &= Q_r^0 + \tilde{Q}_r \\ M_{r\theta} &= M_{r\theta}^0 + \tilde{M}_{r\theta} \end{aligned}\right\} \quad (8\text{-}82)$$

where, when $\frac{a}{h} >> 1$, we have

$$\left.\begin{aligned} \tilde{Q}_r &= -\frac{4}{3+\mu} M_0 \frac{1}{r} \sqrt{\frac{a}{r}} \mathrm{e}^{-\sqrt{10}\left(\frac{r-a}{h}\right)} \cos 2\theta \\ \tilde{M}_{r\theta} &= \frac{2}{3+\mu} M_0 \sqrt{\frac{a}{r}} \mathrm{e}^{-\sqrt{10}\left(\frac{r-a}{h}\right)} \sin 2\theta \end{aligned}\right\} \quad (8\text{-}83)$$

It can be seen that at the boundary $r = a$ of the circular hole, both the boundary conditions $Q_r = 0$ and $M_{r\theta} = 0$ are satisfied indeed.

Let $\tilde{Q}_r$ and $\tilde{M}_{r\theta}$ be the differences $Q_r - Q_r^0$ and $M_{r\theta} - M_{r\theta}^0$ of the solutions from the two theories, respectively. Both $\tilde{Q}_r$ and $\tilde{M}_{r\theta}$ contain the exponential term $\mathrm{e}^{-\sqrt{10}\left(\frac{r-a}{h}\right)}$, which is a rapid attenuation function (refer to Table 8.2). For example, when $\frac{r-a}{h}$ increases from 0 to 1, the function value will decrease from 1 to 4%. Therefore, the solutions of the two theories are discrepant only within a very small neighborhood near the free edge. The scale of this neighborhood belongs to the same magnitude of the thickness h of the plate. Outside the neighborhood, the internal force solutions of the thin plate theory are still suitable.

The solutions of the thick plate theory contain exponential function which will rapidly decay when they are away from the boundary, and this phenomenon is called as edge effect. The solutions (8-81) of the thin plate theory do not contain this type of exponential function, so there is no edge effect phenomenon.

Table 8.2 Exponential function $e^{-\sqrt{10}\left(\frac{r-a}{h}\right)}$

$\frac{r-a}{h}$	0	1/4	1/2	3/4	1	2
$e^{-\sqrt{10}\left(\frac{r-a}{h}\right)}$	1.0000	0.4538	0.2058	0.0933	0.0424	0.0018

7. Contact problem

Consider the beam contact problem shown in Fig. 8.9[3]. The left end of the beam is fixed, and the right free end is subjected to a concentrated load P. Below the beam, there is a circular rigid foundation (the radius is r_1). Under the action of load P, the left segment of the beam ($0 \leqslant x \leqslant x_1$) will contact with the rigid foundation, and the contact length x_1 will increase with P. This is a contact problem.

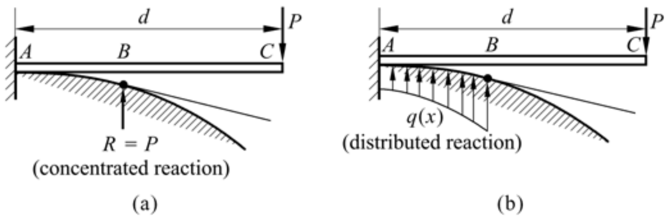

Figure 8.9 Contact problem of beam

(a) Solutions of thin beam theory; (b) Solutions of thick beam theory

Firstly, we solve this problem according to the thin beam theory.

In the contact segment $0 \leqslant x \leqslant x_1$, the deflection is

$$w = \frac{x^2}{2r_1} \tag{8-84}$$

From this equation, we obtain

$$\left.\begin{aligned} &\text{Rotation} && \psi = \frac{\mathrm{d}w}{\mathrm{d}x} = \frac{x}{r_1} \\ &\text{Bending moment} && M = -\frac{D}{r_1} \\ &\text{Shear force} && Q = \frac{\mathrm{d}M}{\mathrm{d}x} = 0 \\ &\text{Distributed reaction} && q = -\frac{\mathrm{d}Q}{\mathrm{d}x} = 0 \end{aligned}\right\} \tag{8-85}$$

Therefore, it can be concluded that the distributed reaction of the contact segment is zero.

In the non-contact segment $x_1 \leqslant x \leqslant d$, the bending moment and shear force can be solved by the equilibrium condition:

$$M = -P(d - x), \quad Q = P \tag{8-86}$$

The length x_1 of the contact segment and the concentrated reaction R can be solved by the static continuity conditions at the interface point B:

$$-P(d - x_1) = -\frac{D}{r_1}, \quad x_1 = d - \frac{D}{Pr_1} \tag{8-87}$$

$$R = P \tag{8-88}$$

Here, another conclusion that there is a concentrated reaction $R = P$ at the interface point B is obtained.

There is no distributed reaction along the whole contact segment, and only a concentrated reaction exists at its end, this strange conclusion is formed completely by ignoring the shear deformation. If this problem is solved according to the thick beam theory, more reasonable results will be obtained.

Secondly, we solve this problem according to the thick beam theory.

The deflection of the contact segment is still expressed by Eq. (8-84). Since the influence of the shear strain γ is considered in the thick beam theory, the ψ, M, Q, q in the contact segment are different from those results by the thin beam theory:

$$\left.\begin{aligned} &\psi = \frac{\mathrm{d}w}{\mathrm{d}x} - \gamma = \frac{x}{r_1} - \gamma \\ &M = -D\frac{\mathrm{d}\psi}{\mathrm{d}x} = -\frac{D}{r_1} + D\frac{\mathrm{d}\gamma}{\mathrm{d}x} \\ &Q = C\gamma \\ &q = -\frac{\mathrm{d}Q}{\mathrm{d}x} = -C\frac{\mathrm{d}\gamma}{\mathrm{d}x} \end{aligned}\right\} \tag{8-89}$$

So, it can be concluded that, there is distributed reaction existing in the contact segment, and it can be derived from the shear strain.

In order to determine the shear strain γ, the equilibrium differential equation $\frac{\mathrm{d}M}{\mathrm{d}x} = Q$ is applied firstly. Substitution of Eq. (8-89) into this equation yields

$$\frac{\mathrm{d}^2\gamma}{\mathrm{d}x^2} - \lambda^2\gamma = 0 \tag{8-90}$$

where

$$\lambda = \sqrt{\frac{C}{D}} \tag{8-91}$$

The solution of Eq. (8-90) is

$$\gamma = \alpha \operatorname{ch} \lambda x + \beta \operatorname{sh} \lambda x \tag{8-92}$$

From the boundary condition $\psi|_{x=0} = 0$ at the left end, we obtain $\gamma|_{x=0} = 0$, $\alpha = 0$, therefore, we have

$$\gamma = \beta \operatorname{sh} \lambda x \tag{8-93}$$

Then, the bending moment and shear force of the contact segment can be obtained as

$$\left.\begin{aligned} M &= -\frac{D}{r_1} + D\beta\lambda \operatorname{ch} \lambda x \\ Q &= C\beta \operatorname{sh} \lambda x \end{aligned}\right\} \tag{8-94}$$

And, the bending moment and shear force of the non-contact segment are still expressed by Eq. (8-86).

By applying the static continuity conditions at point B:

$$\left.\begin{aligned} &-\frac{D}{r_1} + D\beta\lambda \operatorname{ch} \lambda x_1 = -P(d - x_1) \\ &C\beta \operatorname{sh} \lambda x_1 = P \end{aligned}\right\} \tag{8-95}$$

x_1 and β can be solved as follows:

$$\beta = \frac{P}{C \operatorname{sh} \lambda x_1} \tag{8-96}$$

$$\operatorname{cth} \lambda x_1 = \frac{C}{P r_1 \lambda} - \frac{C(d - x_1)}{D\lambda} \tag{8-97}$$

When x_1 is being solved from Eq. (8-97), the trial method can be used.

Finally, the distributed reaction of the contact segment can be obtained as

$$q = -C\beta\lambda \operatorname{ch} \lambda x = -\frac{P\lambda}{\operatorname{sh} \lambda x_1} \operatorname{ch} \lambda x \tag{8-98}$$

in which the positive direction of q is downward.

So, according to the thick beam theory, there is distributed reaction existing in the contact segment, but no concentrated reaction. This conclusion is more reasonable. In contact problem, the influence of the shear strain should not be ignored.

8.3 Thick/Thin Beam Element

8.3.1 The Fundamental Formulae of Thick/Thin Beam Element

A Timoshenko thick beam element is shown in Fig. 8.10. The formulae of deflection w, rotation ψ and shear strain γ are as follows[4]:

$$w = w_i(1-t) + w_j t + \frac{d}{2}(\psi_i - \psi_j)F_2 - \frac{d}{2}\Gamma(1-2\delta)F_3 \tag{8-99a}$$

$$\psi = \psi_i(1-t) + \psi_j t + 3(1-2\delta)\Gamma F_2 \tag{8-99b}$$

$$\gamma = \delta\Gamma \tag{8-99c}$$

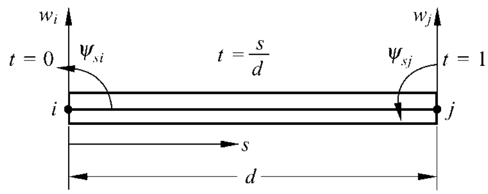

Figure 8.10 Timoshenko thick beam element

where

$$\left.\begin{aligned}
&\Gamma = \frac{2}{d}(-w_i + w_j) - \psi_i - \psi_j \\
&\delta = \frac{6\lambda}{1+12\lambda} = \frac{\left(\dfrac{h}{d}\right)^2}{\dfrac{5}{6}(1-\mu) + 2\left(\dfrac{h}{d}\right)^2} \\
&\lambda = \frac{D}{Cd^2} = \frac{h^2}{5(1-\mu)d^2}, \quad D = \frac{Eh^3}{12(1-\mu^2)}, \quad C = \frac{5}{6}Gh = \frac{5Eh}{12(1+\mu)} \\
&F_2 = t(1-t) \\
&F_3 = t(1-t)(1-2t)
\end{aligned}\right\} \tag{8-100}$$

8.3.2 Derivation of the Fundamental Formulae

Assume that the shear strain γ, rotation ψ and deflection w are constant, quadratic function and cubic function in the beam element, respectively. According to the end conditions, let

$$\left.\begin{aligned}&\gamma=\gamma_0\\&\psi=\psi_i(1-t)+\psi_j t+\alpha_0 t(1-t)\\&w=w_i(1-t)+w_j t+\beta_0 dt(1-t)+\beta_1 dt(1-t)(1-2t)\end{aligned}\right\}\tag{8-101}$$

γ, ψ, w should satisfy the following equation:

$$\frac{\mathrm{d}w}{d\mathrm{d}t}-\psi=\gamma\tag{8-102}$$

Substitution of Eq. (8-101) into Eq. (8-102) yields

$$\beta_0=\frac{1}{2}(\psi_1-\psi_2),\quad \beta_1=\gamma_0-\frac{1}{2}\varGamma,\quad \alpha_0=-6\left(\gamma_0-\frac{1}{2}\varGamma\right)\tag{8-103}$$

Substitution of Eq. (8-103) into Eq. (8-101) yields

$$\left.\begin{aligned}&\gamma=\gamma_0\\&\psi=\psi_i(1-t)+\psi_j t-6\left(\gamma_0-\frac{1}{2}\varGamma\right)t(1-t)\\&w=w_i(1-t)+w_j t+\frac{d}{2}(\psi_i-\psi_j)t(1-t)+d\left(\gamma_0-\frac{1}{2}\varGamma\right)t(1-t)(1-2t)\end{aligned}\right\}\tag{8-104}$$

in which γ_0 is an internal parameter which can be determined from the condition of minimum strain energy.

Curvature:

$$\kappa=-\frac{\mathrm{d}\psi}{d\mathrm{d}t}=\frac{1}{d}\left[\psi_i-\psi_j+6\left(\gamma_0-\frac{1}{2}\varGamma\right)(1-2t)\right]=\kappa^0+\frac{6\gamma_0}{d}(1-2t)$$

$$\kappa^0=\frac{1}{d}[\psi_i-\psi_j-3\varGamma(1-2t)]$$

Bending strain energy:

$$\begin{aligned}U_{\mathrm{b}}&=\frac{Dd}{2}\int_0^1\kappa^2\mathrm{d}t=\frac{Dd}{2}\int_0^1\left[(\kappa^0)^2+\frac{12\gamma_0}{d}\kappa^0(1-2t)+\frac{36\gamma_0^2}{d^2}(1-2t)^2\right]\mathrm{d}t\\&=U_{\mathrm{b}}^0-\frac{6D}{d}(\gamma_0\varGamma-\gamma_0^2)\end{aligned}$$

in which

$$U_{\mathrm{b}}^0=\frac{Dd}{2}\int_0^1(\kappa^0)^2\mathrm{d}t$$

Shear strain energy:

$$U_{\mathrm{s}} = \frac{Cd}{2}\gamma_0^2$$

The strain energy:

$$U = U_{\mathrm{b}} + U_{\mathrm{s}} = U_{\mathrm{b}}^0 - \frac{6D\gamma_0}{d}\mathit{\Gamma} + \frac{D}{2d}\left(12 + \frac{1}{\lambda}\right)\gamma_0^2 \tag{8-105}$$

From $\dfrac{\partial U}{\partial \gamma_0} = 0$, we have:

$$\gamma_0 = \frac{6\lambda}{1+12\lambda}\mathit{\Gamma} = \delta\mathit{\Gamma} \tag{8-106}$$

Substitution of Eq. (8-106) into Eq. (8-104) yields Eq. (8-99).

8.3.3 The Stiffness Matrix of Thick/Thin Beam Element

The stiffness matrix $\boldsymbol{K}^e$ of the thick/thin beam element can be derived from the element strain energy *U*:

$$U = \frac{1}{2}\boldsymbol{q}^{e\mathrm{T}}\boldsymbol{K}^e\boldsymbol{q}^e \tag{8-107}$$

Substitution of Eq. (8-106) into Eq. (8-105) yields the expression of the strain energy as follows:

$$U = U_{\mathrm{b}}^0 + \Delta U \tag{8-108}$$

where U_{b}^0 is the strain energy of the thin beam element, and the strain energy increment ΔU is

$$\Delta U = -\frac{3D}{d}\delta\mathit{\Gamma}^2 \tag{8-109}$$

The stiffness matrix $\boldsymbol{K}^e$ of the thick/thin beam element can be written as the sum of two terms:

$$\boldsymbol{K}^e = \boldsymbol{K}^{0e} + \Delta\boldsymbol{K} \tag{8-110}$$

where $\boldsymbol{K}^{0e}$ is the stiffness of the thin beam element, and by

$$U_{\mathrm{b}}^0 = \frac{1}{2}\boldsymbol{q}^{e\mathrm{T}}\boldsymbol{K}^{0e}\boldsymbol{q}^e$$

we have

$$\boldsymbol{K}^{0e} = \frac{2D}{d^3}\begin{bmatrix} 6 & 3d & -6 & 3d \\ 3d & 2d^2 & -3d & d^2 \\ -6 & -3d & 6 & -3d \\ 3d & d^2 & -3d & 2d^2 \end{bmatrix} \tag{8-111}$$

And, the incremental matrix $\Delta\boldsymbol{K}$ can be determined by

$$\Delta U = \frac{1}{2}\boldsymbol{q}^{e\mathrm{T}}\Delta\boldsymbol{K}\boldsymbol{q}^e$$

i.e.,

$$\Delta\boldsymbol{K} = -\frac{6D}{d^3}\delta\begin{bmatrix} 4 & 2d & -4 & 2d \\ 2d & d^2 & -2d & d^2 \\ -4 & -2d & 4 & -2d \\ 2d & d^2 & -2d & d^2 \end{bmatrix} \tag{8-112}$$

When the thickness-span ratio $\frac{h}{d}$ decreases gradually, the following limitation relation can be obtained:

$$\delta \to 0, \quad \Delta\boldsymbol{K} \to \boldsymbol{0}, \quad \boldsymbol{K}^e \to \boldsymbol{K}^{0e}$$

Here, the stiffness matrix $\boldsymbol{K}^e$ of the thick/thin beam element automatically degenerates to be the stiffness matrix $\boldsymbol{K}^{0e}$ of the thin beam element. Therefore, no shear locking will happen.

8.4 Review of Displacement-based Thick/Thin Plate Elements

This section will present a brief review of the construction methods of the displacement-based thick/thin plate elements.

The construction methods of the displacement-based thick/thin plate elements are mainly classified into two types: One starts with the thick plate theory, and uses the procedure of transition from the thick plate element to the thick/thin plate element, which is simply denoted as *thick-to-thin scheme* here; the other starts with the thin plate theory, and uses the procedure of transition from the thin plate element to the thin/thick plate element, which is simply denoted as *thin-to-thick scheme* here.

Further explanations are given as follows.

8.4.1 Thick-to-Thin Scheme

The element suitable for the thick plates is firstly constructed based on the thick plate theory; and then, some special treatments are adopted so that the element will satisfy the requirements of the thin plate theory in the thin plate cases.

When constructing the thick plate element, it can be started with assuming the displacement and shear strain fields. In the three variable fields, i.e., the deflection field w, rotation field $\boldsymbol{\psi}$ and shear strain field $\boldsymbol{\gamma}$, two of them can be selected to be interpolated rationally, and then the third one can be derived from Eq. (8-1). Since there are three combination forms (w, $\boldsymbol{\psi}$), ($\boldsymbol{\psi}$, $\boldsymbol{\gamma}$) and (w, $\boldsymbol{\gamma}$) available, accordingly, the corresponding three different schemes are presented. Among these three schemes, the first one which starts with assuming (w, $\boldsymbol{\psi}$) is the traditional scheme of assuming displacements and is often used in literatures, and the other two are the approaches proposed recently—mixed interpolation schemes partly of displacement and partly of strain.

(1) Scheme starting with assuming (w, $\boldsymbol{\psi}$)

For the thick plate case, w and $\boldsymbol{\psi}$ should be independent variables; when the plate degenerates to be a thin plate, $\boldsymbol{\psi}$ should be the derivatives of w and not be independent variables anymore. Therefore, the rational assumptions of w and $\boldsymbol{\psi}$ should fulfill the twofold requirements: independence in the thick plate case and non-independence in the thin plate case. This is the main difficulty encountered by this scheme.

In fact, some elements constructed by this scheme possess good precision for the analysis of the thick plates, but an over-stiff performance is obviously exhibited when analyzing the thin plates, i.e., the computational results of deflections are much smaller than correct solutions. This is the shear locking phenomenon. The reason leading to shear locking is that the dual requirements mentioned above are not satisfied when assuming w and $\boldsymbol{\psi}$, consequently, false shear strain will appear in the thin plate limit state. How to avoid shear locking phenomenon was one of the problems that attracted continuous attention from academia, and many modifications and numerical techniques have been proposed by numerous researchers, such as the reduced integration method[5], the selective reduced integration method[6], the substitute shear strain method[7], and so on.

(2) Scheme starting with assuming ($\boldsymbol{\psi}$, $\boldsymbol{\gamma}$)

In order to avoid the difficulty mentioned above caused by assuming (w, $\boldsymbol{\psi}$), the scheme of assuming ($\boldsymbol{\psi}$, $\boldsymbol{\gamma}$) can be used to replace it. For a rational assumption of the shear strain $\boldsymbol{\gamma}$, the dual requirements, that $\boldsymbol{\gamma}$ should be generally nonzero in the thick plate case and tend to be zero in the thin plate case, should be still paid attention to. But then, these dual requirements are much easier to be satisfied, which provides a new way for eliminating shear locking. Some related research achievements[4,8,9] will be introduced in Sect. 8.5.

By the way, the discrete Kirchhoff theory (DKT) elements for the thin plates indeed belong to a special application of the above scheme.

(3) Scheme starting with assuming (w, γ)

This is another new scheme[10,11] which can eliminate shear locking, and will be introduced in Sect. 8.6.

8.4.2 Thin-to-Thick Scheme

The element suitable for the thin plates is firstly constructed based on the thin plate theory; and then, some special treatments are adopted so that the influences of shear strain are introduced, thus, the thin plate element is generalized to an element suitable for both thin and thick plates. The shear strain introduced here should automatically degenerate to be zero in the thin plate limit state. Hence, naturally, the elements according to this scheme will not suffer from shear locking phenomenon.

Some high-quality thin plate elements have already been proposed in literatures. Starting with these elements, the corresponding thin/thick plate elements can be constructed by this scheme.

Some related research achievements will be introduced in Sect. 8.7.

By the way, there is another effective method, namely, the Analytical Trial Function (ATF) method, for constructing the universal elements for both thick and thin plates[12]. This will be introduced in Chap. 14.

8.5 Generalized Conforming Thick/Thin Plate Elements (1) —Starting with Assuming (ψ ,γ)

This section will introduce the construction procedure of the thick/thin plate elements starting with assuming (ψ ,γ)[4,8,9]. The derivation of the triangular element in reference [4] is quite simple and straightforward, and possesses clear physical meaning. So, the procedure in [4] will be introduced here. And, the method of deriving quadrilateral element can be referred to [9].

Main procedure: The functions of rotation and shear strain along each side of the element are firstly determined using the Timoshenko beam theory; Secondly, the rotation and shear strain fields in the domain of the element are then determined using the technique of improved interpolation, and the curvature fields are then determined from the rotation fields; Finally, the element stiffness matrix is determined by the curvature and shear strain fields. This new element is denoted by TMT (Timoshenko-Mindlin Triangular element).

When the thickness becomes small, the thick beam theory will automatically degenerate to be the thin beam theory, and then the shear strain along each element side and the interpolation formulas for shear strain in the domain of the element will all automatically degenerate to be zero. So, the element TMT will automatically degenerate to be the thin plate element, no shear locking will happen.

8.5.1 Interpolation Formulas for the Rotation Fields of the Thick Plate Element

Consider the triangular thick plate element shown in Fig. 8.11. The element has 3 nodes and 3 engineering DOFs per node. The element nodal displacement vector is:

$$\boldsymbol{q}^e = [w_1 \quad \psi_{x1} \quad \psi_{y1} \quad w_2 \quad \psi_{x2} \quad \psi_{y2} \quad w_3 \quad \psi_{x3} \quad \psi_{y3}]^{\mathrm{T}}$$

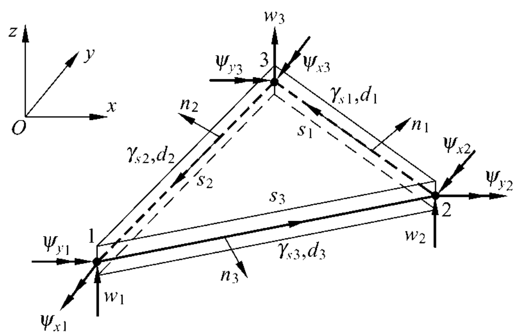

Figure 8.11 A triangular thick plate element

The interpolation formulas for the element rotation fields can be obtained by the rotation formulas along each element side.

1. Formulas of normal rotation ψ_n and tangential rotation ψ_s along each side

The variation of the normal rotation ψ_n along each side is assumed to be linear. For the three sides ($\overline{23},\overline{31},\overline{12}$), we have

$$\left.\begin{aligned} \psi_{n23} &= (\psi_{n23})_2 L_2 + (\psi_{n23})_3 L_3 \\ \psi_{n31} &= (\psi_{n31})_3 L_3 + (\psi_{n31})_1 L_1 \\ \psi_{n12} &= (\psi_{n12})_1 L_1 + (\psi_{n12})_2 L_2 \end{aligned}\right\} \tag{8-113a}$$

The variation of the tangential rotation ψ_s along each side can be determined by Eq. (8-99b). Thus,

$$\left.\begin{aligned} \psi_{s23} &= (\psi_{s23})_2 L_2 + (\psi_{s23})_3 L_3 + 3(1-2\delta_1)\Gamma_1 L_2 L_3 \\ \psi_{s31} &= (\psi_{s31})_3 L_3 + (\psi_{s31})_1 L_1 + 3(1-2\delta_2)\Gamma_2 L_3 L_1 \\ \psi_{s12} &= (\psi_{s12})_1 L_1 + (\psi_{s12})_2 L_2 + 3(1-2\delta_3)\Gamma_3 L_1 L_2 \end{aligned}\right\} \tag{8-113b}$$

where

$$\left.\begin{aligned}
&\delta_i = \frac{\left(\dfrac{h}{d_i}\right)^2}{2\left(\dfrac{h}{d_i}\right)^2 + \dfrac{5}{6}(1-\mu)} \quad (i=1,2,3) \\
&\varGamma_i = \frac{1}{d_i}[2(-w_j + w_k) - c_i(\psi_{xj} + \psi_{xk}) + b_i(\psi_{yj} + \psi_{yk})] \\
&b_i = y_j - y_k \quad (\overrightarrow{\underleftarrow{i,j,k}} = \overrightarrow{\underleftarrow{1,2,3}}) \\
&c_i = x_k - x_j
\end{aligned}\right\} \tag{8-114}$$

2. Expressions of rotations ψ_x and ψ_y along each side

By using the relation between (ψ_n, ψ_s) and (ψ_x, ψ_y), the expression of rotations ψ_x and ψ_y can be obtained as follows:

$$\left.\begin{aligned}
&\psi_{x23} = -\frac{1}{d_1}(b_1\psi_{n23} - c_1\psi_{s23}) = \psi_{x2}L_2 + \psi_{x3}L_3 + \frac{3c_1}{d_1}(1-2\delta_1)\varGamma_1 L_2 L_3 \\
&\psi_{x31} = \psi_{x3}L_3 + \psi_{x1}L_1 + \frac{3c_2}{d_2}(1-2\delta_2)\varGamma_2 L_3 L_1 \\
&\psi_{x12} = \psi_{x1}L_1 + \psi_{x2}L_2 + \frac{3c_3}{d_3}(1-2\delta_3)\varGamma_3 L_1 L_2
\end{aligned}\right\} \tag{8-115a}$$

$$\left.\begin{aligned}
&\psi_{y23} = -\frac{1}{d_1}(c_1\psi_{n23} + b_1\psi_{s23}) = \psi_{y2}L_2 + \psi_{y3}L_3 - \frac{3b_1}{d_1}(1-2\delta_1)\varGamma_1 L_2 L_3 \\
&\psi_{y31} = \psi_{y3}L_3 + \psi_{y1}L_1 - \frac{3b_2}{d_2}(1-2\delta_2)\varGamma_2 L_3 L_1 \\
&\psi_{y12} = \psi_{y1}L_1 + \psi_{y2}L_2 - \frac{3b_3}{d_3}(1-2\delta_3)\varGamma_3 L_1 L_2
\end{aligned}\right\} \tag{8-115b}$$

3. Interpolation formulas for element rotation fields ψ_x and ψ_y

The rotation fields ψ_x and ψ_y within the element can then be obtained by the interpolation of the expressions (8-115a,b) of ψ_x and ψ_y on each side, i.e.

$$\left.\begin{aligned}
\psi_x = {} & \psi_{x1}L_1 + \psi_{x2}L_2 + \psi_{x3}L_3 + \frac{3c_1}{d_1}(1-2\delta_1)\varGamma_1 L_2 L_3 \\
& + \frac{3c_2}{d_2}(1-2\delta_2)\varGamma_2 L_3 L_1 + \frac{3c_3}{d_3}(1-2\delta_3)\varGamma_3 L_1 L_2 \\
\psi_y = {} & \psi_{y1}L_1 + \psi_{y2}L_2 + \psi_{y3}L_3 - \frac{3b_1}{d_1}(1-2\delta_1)\varGamma_1 L_2 L_3 \\
& - \frac{3b_2}{d_2}(1-2\delta_2)\varGamma_2 L_3 L_1 - \frac{3b_3}{d_3}(1-2\delta_3)\varGamma_3 L_1 L_2
\end{aligned}\right\} \tag{8-116}$$

It can be seen that, if $L_i = 0$, the expressions of element rotations ψ_x and ψ_y obtained from the above equation are the same as those expressions of rotations along each side given in (8-115a,b). That is to say, The interpolation formulas (8-116) for element rotations are exactly compatible with the formulas (8-115a,b) for rotations along each side.

8.5.2 The Curvature Fields of the Thick Plate Element

The element curvature fields are

$$\boldsymbol{\kappa} = [\kappa_x \quad \kappa_y \quad 2\kappa_{xy}]^{\mathrm{T}} = \left[-\frac{\partial \psi_x}{\partial x} \quad -\frac{\partial \psi_y}{\partial y} \quad -\left(\frac{\partial \psi_x}{\partial y} + \frac{\partial \psi_y}{\partial x} \right) \right]^{\mathrm{T}} \tag{8-117}$$

By using the differential formulae:

$$\left.\begin{aligned} \frac{\partial}{\partial x} &= \frac{1}{2A}\left(b_1 \frac{\partial}{\partial L_1} + b_2 \frac{\partial}{\partial L_2} + b_3 \frac{\partial}{\partial L_3} \right) \\ \frac{\partial}{\partial y} &= \frac{1}{2A}\left(c_1 \frac{\partial}{\partial L_1} + c_2 \frac{\partial}{\partial L_2} + c_3 \frac{\partial}{\partial L_3} \right) \end{aligned}\right\} \tag{8-118}$$

and substituting Eq. (8-116) into Eq. (8-117), we obtain

$$\left.\begin{aligned} \kappa_x &= -\frac{1}{2A}[b_1\psi_{x1} + b_2\psi_{x2} + b_3\psi_{x3} + \frac{3(1-2\delta_1)\Gamma_1}{d_1} c_1(b_2L_3 + b_3L_2) \\ &\quad + \frac{3(1-2\delta_2)\Gamma_2}{d_2} c_2(b_3L_1 + b_1L_3) + \frac{3(1-2\delta_3)\Gamma_3}{d_3} c_3(b_1L_2 + b_2L_1)] \\ \kappa_y &= -\frac{1}{2A}[c_1\psi_{y1} + c_2\psi_{y2} + c_3\psi_{y3} - \frac{3(1-2\delta_1)\Gamma_1}{d_1} b_1(c_2L_3 + c_3L_2) \\ &\quad - \frac{3(1-2\delta_2)\Gamma_2}{d_2} b_2(c_3L_1 + c_1L_3) - \frac{3(1-2\delta_3)\Gamma_3}{d_3} b_3(c_1L_2 + c_2L_1)] \\ 2\kappa_{xy} &= -\frac{1}{2A}(c_1\psi_{x1} + c_2\psi_{x2} + c_3\psi_{x3} + b_1\psi_{y1} + b_2\psi_{y2} + b_3\psi_{y3} + E_1 + E_2 + E_3) \end{aligned}\right\} \tag{8-119}$$

where

$$\left.\begin{aligned} E_1 &= \frac{3(1-2\delta_1)\Gamma_1}{d_1}[(c_1c_2 - b_1b_2)L_3 + (c_3c_1 - b_3b_1)L_2] \\ E_2 &= \frac{3(1-2\delta_2)\Gamma_2}{d_2}[(c_2c_3 - b_2b_3)L_1 + (c_1c_2 - b_1b_2)L_3] \\ E_3 &= \frac{3(1-2\delta_3)\Gamma_3}{d_3}[(c_3c_1 - b_3b_1)L_2 + (c_2c_3 - b_2b_3)L_1] \end{aligned}\right\} \tag{8-120}$$

Equation (8-119) can be written as

$$\boldsymbol{\kappa} = \boldsymbol{B}_{\mathrm{b}}\boldsymbol{q}^e \tag{8-121}$$

where

$$\boldsymbol{B}_{\mathrm{b}} = \boldsymbol{B}_{\mathrm{b}}^0 + \boldsymbol{F}\boldsymbol{\Delta}\tilde{\boldsymbol{G}} \tag{8-122}$$

$$\boldsymbol{B}_{\mathrm{b}}^0 = -\frac{1}{2A}\begin{bmatrix} 0 & b_1 & 0 & 0 & b_2 & 0 & 0 & b_3 & 0 \\ 0 & 0 & c_1 & 0 & 0 & c_2 & 0 & 0 & c_3 \\ 0 & c_1 & b_1 & 0 & c_2 & b_2 & 0 & c_3 & b_3 \end{bmatrix} \tag{8-123}$$

$$\boldsymbol{F} = -\frac{3}{2A}\begin{bmatrix} \frac{c_1}{d_1^2}(b_2L_3 + b_3L_2) & \frac{c_2}{d_2^2}(b_3L_1 + b_1L_3) & \frac{c_3}{d_3^2}(b_1L_2 + b_2L_1) \\ -\frac{b_1}{d_1^2}(c_2L_3 + c_3L_2) & -\frac{b_2}{d_2^2}(c_3L_1 + c_1L_3) & -\frac{b_3}{d_3^2}(c_1L_2 + c_2L_1) \\ M_1 & M_2 & M_3 \end{bmatrix} \tag{8-124}$$

$$\left.\begin{aligned} M_1 &= \frac{1}{d_1^2}[(c_1c_2 - b_1b_2)L_3 + (c_3c_1 - b_3b_1)L_2] \\ M_2 &= \frac{1}{d_2^2}[(c_2c_3 - b_2b_3)L_1 + (c_1c_2 - b_1b_2)L_3] \\ M_3 &= \frac{1}{d_3^2}[(c_3c_1 - b_3b_1)L_2 + (c_2c_3 - b_2b_3)L_1] \end{aligned}\right\} \tag{8-125}$$

$$\boldsymbol{\Delta} = \begin{bmatrix} 1-2\delta_1 & 0 & 0 \\ 0 & 1-2\delta_2 & 0 \\ 0 & 0 & 1-2\delta_3 \end{bmatrix} \tag{8-126}$$

$$\tilde{\boldsymbol{G}} = \begin{bmatrix} 0 & 0 & 0 & -2 & -c_1 & b_1 & 2 & -c_1 & b_1 \\ 2 & -c_2 & b_2 & 0 & 0 & 0 & -2 & -c_2 & b_2 \\ -2 & -c_3 & b_3 & 2 & -c_3 & b_3 & 0 & 0 & 0 \end{bmatrix} \tag{8-127}$$

8.5.3 Interpolation Formulas for Shear Strain Fields of the Thick Plate Element

1. Shear strain along each element side

The transverse shear strain γ_s along the tangential direction (s-direction) of each side is constant. From Eq. (8-99c), we obtain

$$\gamma_{s23} = \delta_1 \Gamma_1, \quad \gamma_{s31} = \delta_2 \Gamma_2, \quad \gamma_{s12} = \delta_3 \Gamma_3 \tag{8-128}$$

in which δ_i and Γ_i are given by Eq. (8-114).

On the boundary line $L_i = 0$, the transformation relations between shear strain components (γ_n, γ_s) and (γ_x, γ_y) are

$$\begin{Bmatrix} \gamma_n \\ \gamma_s \end{Bmatrix}_{L_i=0} = \frac{1}{d_i} \begin{bmatrix} -b_i & -c_i \\ c_i & -b_i \end{bmatrix} \begin{Bmatrix} \gamma_x \\ \gamma_y \end{Bmatrix}_{L_i=0} \tag{8-129}$$

Then, γ_s along each side can be expressed in terms of γ_x and γ_y as follows

$$\left.\begin{aligned} d_1 \gamma_{s23} &= c_1 \gamma_{x23} - b_1 \gamma_{y23} \\ d_2 \gamma_{s31} &= c_2 \gamma_{x31} - b_2 \gamma_{y31} \\ d_3 \gamma_{s12} &= c_3 \gamma_{x12} - b_3 \gamma_{y12} \end{aligned}\right\} \tag{8-130}$$

2. Determination of nodal shear strains γ_{xi} and γ_{yi}

Firstly, consider node 1.

There are two sides, $\overline{31}$ and $\overline{12}$, meeting at node 1. According to Eq. (8-130), the tangential shear strains γ_{s31} and γ_{s12} along these two sides can be expressed by the shear strains γ_{x1} and γ_{y1} at node 1, i.e.,

$$\begin{Bmatrix} d_2 \gamma_{s31} \\ d_3 \gamma_{s12} \end{Bmatrix} = \begin{bmatrix} c_2 & -b_2 \\ c_3 & -b_3 \end{bmatrix} \begin{Bmatrix} \gamma_{x1} \\ \gamma_{y1} \end{Bmatrix}$$

Then, we obtain

$$\begin{Bmatrix} \gamma_{x1} \\ \gamma_{y1} \end{Bmatrix} = \frac{1}{2A} \begin{bmatrix} -b_3 & b_2 \\ -c_3 & c_2 \end{bmatrix} \begin{Bmatrix} d_2 \gamma_{s31} \\ d_3 \gamma_{s12} \end{Bmatrix} = \frac{1}{2A} \begin{bmatrix} -b_3 & b_2 \\ -c_3 & c_2 \end{bmatrix} \begin{Bmatrix} d_2 \delta_2 \Gamma_2 \\ d_3 \delta_3 \Gamma_3 \end{Bmatrix} \tag{8-131}$$

Similarly, for nodes 2 and 3, we have

$$\left.\begin{aligned} \begin{Bmatrix} \gamma_{x2} \\ \gamma_{y2} \end{Bmatrix} &= \frac{1}{2A} \begin{bmatrix} -b_1 & b_3 \\ -c_1 & c_3 \end{bmatrix} \begin{Bmatrix} d_3 \delta_3 \Gamma_3 \\ d_1 \delta_1 \Gamma_1 \end{Bmatrix} \\ \begin{Bmatrix} \gamma_{x3} \\ \gamma_{y3} \end{Bmatrix} &= \frac{1}{2A} \begin{bmatrix} -b_2 & b_1 \\ -c_2 & c_1 \end{bmatrix} \begin{Bmatrix} d_1 \delta_1 \Gamma_1 \\ d_2 \delta_2 \Gamma_2 \end{Bmatrix} \end{aligned}\right\} \tag{8-132}$$

Thus, from Eqs. (8-131) and (8-132), we obtain

$$\begin{Bmatrix} \gamma_{x1} \\ \gamma_{x2} \\ \gamma_{x3} \end{Bmatrix} = \frac{1}{2A} \begin{bmatrix} 0 & -b_3 & b_2 \\ b_3 & 0 & -b_1 \\ -b_2 & b_1 & 0 \end{bmatrix} \begin{Bmatrix} d_1 \delta_1 \Gamma_1 \\ d_2 \delta_2 \Gamma_2 \\ d_3 \delta_3 \Gamma_3 \end{Bmatrix} \tag{8-133}$$

$$\begin{Bmatrix} \gamma_{y1} \\ \gamma_{y2} \\ \gamma_{y3} \end{Bmatrix} = \frac{1}{2A} \begin{bmatrix} 0 & -c_3 & c_2 \\ c_3 & 0 & -c_1 \\ -c_2 & c_1 & 0 \end{bmatrix} \begin{Bmatrix} d_1\delta_1\Gamma_1 \\ d_2\delta_2\Gamma_2 \\ d_3\delta_3\Gamma_3 \end{Bmatrix} \tag{8-134}$$

3. Interpolation formulas for element shear strain fields

The shear strain fields within the element can be obtained in terms of the nodal shear strains in the following manner

$$\left.\begin{aligned} \gamma_x &= \gamma_{x1}L_1 + \gamma_{x2}L_2 + \gamma_{x3}L_3 \\ \gamma_y &= \gamma_{y1}L_1 + \gamma_{y2}L_2 + \gamma_{y3}L_3 \end{aligned}\right\} \tag{8-135}$$

in which the nodal shear strains are given by Eqs.(8-133) and (8-134). After substituting these into the above equation, we obtain

$$\boldsymbol{\gamma} = \begin{Bmatrix} \gamma_x \\ \gamma_y \end{Bmatrix} = \boldsymbol{H} \begin{Bmatrix} \delta_1 d_1 \Gamma_1 \\ \delta_2 d_2 \Gamma_2 \\ \delta_3 d_3 \Gamma_3 \end{Bmatrix} \tag{8-136}$$

where

$$\boldsymbol{H} = \frac{1}{2A} \begin{bmatrix} b_3L_2 - b_2L_3 & b_1L_3 - b_3L_1 & b_2L_1 - b_1L_2 \\ c_3L_2 - c_2L_3 & c_1L_3 - c_3L_1 & c_2L_1 - c_1L_2 \end{bmatrix} \tag{8-137}$$

Equation (8-136) can also be written as

$$\boldsymbol{\gamma} = \boldsymbol{B}_s \boldsymbol{q}^e \tag{8-138}$$

where

$$\boldsymbol{B}_s = \boldsymbol{H}\boldsymbol{\Delta}'\tilde{\boldsymbol{G}} \tag{8-139}$$

$$\boldsymbol{\Delta}' = \begin{bmatrix} \delta_1 & 0 & 0 \\ 0 & \delta_2 & 0 \\ 0 & 0 & \delta_3 \end{bmatrix}$$

$\tilde{\boldsymbol{G}}$ is given by Eq. (8-127).

4. Expression in Cartesian coordinates for shear strains of the triangular element

For the triangular element, the shear strains γ_x and γ_y are determined by 3 constant shear strains $(\gamma_s)_{12}, (\gamma_s)_{23}, (\gamma_s)_{31}$ along 3 sides, therefore, the general expressions of γ_x and γ_y can be written as

$$\left.\begin{aligned}\gamma_x &= \gamma_1 + \gamma_3 y \\ \gamma_y &= \gamma_2 - \gamma_3 x\end{aligned}\right\} \tag{8-140}$$

in which 3 parameters γ_1, γ_2 and γ_3 are involved. This equation can be proved as follows.

For side $\overline{12}$, the shear strain $(\gamma_s)_{12}$ along the side can be expressed by the shear strains at the end point (γ_{x1}, γ_{y1}) or (γ_{x2}, γ_{y2}), as shown in the following Eq. (a)

$$d_3\gamma_{s12} = c_3\gamma_{x1} - b_3\gamma_{y1} = c_3\gamma_{x2} - b_3\gamma_{y2} \tag{a}$$

$$d_1\gamma_{s23} = c_1\gamma_{x2} - b_1\gamma_{y2} = c_1\gamma_{x3} - b_1\gamma_{y3} \tag{b}$$

$$d_2\gamma_{s31} = c_2\gamma_{x3} - b_2\gamma_{y3} = c_2\gamma_{x1} - b_2\gamma_{y1} \tag{c}$$

Equations (b) and (c) can be obtained similarly.

Temporarily assume that γ_x and γ_y are the complete linear polynomials:

$$\left.\begin{aligned}\gamma_x &= \alpha_0 + \alpha_1 x + \alpha_2 y \\ \gamma_y &= \beta_0 + \beta_1 x + \beta_2 y\end{aligned}\right\} \tag{d}$$

in which 6 unknown coefficients are contained. Substitution of Eq. (d) into Eqs. (a), (b), (c) yields

$$\begin{bmatrix} c_3^2 & b_3^2 & -b_3c_3 \\ c_1^2 & b_1^2 & -b_1c_1 \\ c_2^2 & b_2^2 & -b_2c_2 \end{bmatrix} \begin{Bmatrix} \alpha_1 \\ \beta_2 \\ \alpha_2 + \beta_1 \end{Bmatrix} = \begin{Bmatrix} 0 \\ 0 \\ 0 \end{Bmatrix} \tag{e}$$

Since the determinant of the coefficient matrix at the left side is $(2A)^3$, not zero, so, we obtain

$$\alpha_1 = 0, \quad \beta_2 = 0, \quad \alpha_2 = -\beta_1 \tag{f}$$

From Eq. (d), we have

$$\left.\begin{aligned}\gamma_x &= \alpha_0 + \alpha_2 y \\ \gamma_y &= \beta_0 - \alpha_2 x\end{aligned}\right\} \tag{g}$$

Equation (g) is just the form of Eq. (8-140). QED.

By the way, if $\boldsymbol{H}$ in Eq. (8-137) is expressed in the Cartesian coordinates, the shear strain formulas (8-136) can be expressed by the form of Eq. (8-140).

8.5.4 Stiffness Matrix of the Thick Plate

The element stiffness matrix $\boldsymbol{K}^e$ is composed of two parts

$$\boldsymbol{K}^e = \boldsymbol{K}_\mathrm{b}^{\,e} + \boldsymbol{K}_\mathrm{s}^{\,e} \tag{8-141}$$

where $\boldsymbol{K}_\mathrm{b}^{\,e}$ is the bending stiffness matrix:

$$\boldsymbol{K}_\mathrm{b}^{\,e} = \iint_{A^e} \boldsymbol{B}_\mathrm{b}^\mathrm{T} \boldsymbol{D}_\mathrm{b} \boldsymbol{B}_\mathrm{b} \mathrm{d}A \tag{8-142}$$

$\boldsymbol{B}_\mathrm{b}$ is given by Eq. (8-122), $\boldsymbol{D}_\mathrm{b}$ is the bending elastic matrix:

$$\boldsymbol{D}_\mathrm{b} = D\begin{bmatrix} 1 & \mu & 0 \\ \mu & 1 & 0 \\ 0 & 0 & \dfrac{1-\mu}{2} \end{bmatrix}, \quad D = \frac{Eh^3}{12(1-\mu^2)} \tag{8-143}$$

$\boldsymbol{K}_\mathrm{s}^{\,e}$ is the shear stiffness matrix:

$$\boldsymbol{K}_\mathrm{s}^{\,e} = \iint_{A^e} \boldsymbol{B}_\mathrm{s}^\mathrm{T} \boldsymbol{D}_\mathrm{s} \boldsymbol{B}_\mathrm{s} \mathrm{d}A \tag{8-144}$$

$\boldsymbol{B}_\mathrm{s}$ is given by Eq. (8-139), $\boldsymbol{D}_\mathrm{s}$ is the shear elastic matrix:

$$\boldsymbol{D}_\mathrm{s} = C\begin{bmatrix} 1 & 0 \\ 0 & 1 \end{bmatrix}, \quad C = \frac{5}{6}Gh \tag{8-145}$$

8.5.5 Numerical Examples

Example 8.1 The central deflection and moment of simply-supported (hard) square plates with different thickness-span ratios (*h/L*) subjected to uniform load.

Assume that the side length of the plate is *L*, $\mu = 0.3$. Meshes *A* and *B* in Fig. 8.12 are used. The results by the element TMT are given in Tables 8.3 to 8.5.

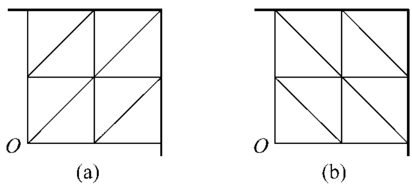

Figure 8.12 Meshes for 1/4 square plate (*O* is the center of the plate)
(a) Mesh *A* 2 × 2; (b) Mesh *B* 2 × 2

Table 8.3 The central deflection of simply-supported square plates subjected to uniform load $q\Big/\left(\dfrac{qL^4}{100D}\right)$

h/L \ Mesh type \ Mesh number		2×2	4×4	8×8	16×16	Analytical
10^{-30}	*A* *B*	0.4056 0.3676	0.4065 0.3973	0.4064 0.4041	0.4063 0.4057	0.4062
0.001	*A* *B*	0.4056 0.3676	0.4065 0.3973	0.4064 0.4041	0.4063 0.4057	0.4062
0.01	*A* *B*	0.4058 0.3677	0.4066 0.3974	0.4065 0.4042	0.4064 0.4059	0.4064
0.1	*A* *B*	0.4255 0.3845	0.4264 0.4164	0.4270 0.4244	0.4272 0.4266	0.4273
0.15	*A* *B*	0.4520 0.4063	0.4529 0.4414	0.4534 0.4504	0.4536 0.4528	0.4536
0.20	*A* *B*	0.4902 0.4370	0.4905 0.4764	0.4906 0.4867	0.4905 0.4895	0.4906
0.25	*A* *B*	0.5398 0.4769	0.5388 0.5215	0.5383 0.5334	0.5380 0.5366	0.5379
0.30	*A* *B*	0.6009 0.5257	0.5979 0.5767	0.5966 0.5905	0.5960 0.5943	0.5956
0.35	*A* *B*	0.6732 0.5835	0.6679 0.6418	0.6655 0.6580	0.6646 0.6624	0.6641

Table 8.4 The central deflection of clamped square plates subjected to uniform load $q\Big/\left(\dfrac{qL^4}{100D}\right)$

h/L \ Mesh type \ Mesh number		2×2	4×4	8×8	16×16	Analytical
10^{-30}	*A* *B*	0.1547 0.1214	0.1347 0.1258	0.1287 0.1264	0.1271 0.1265	0.1265
0.001	*A* *B*	0.1547 0.1214	0.1347 0.1258	0.1287 0.1264	0.1271 0.1265	0.1265
0.01	*A* *B*	0.1550 0.1216	0.1350 0.1260	0.1289 0.1266	0.1273 0.1267	0.1265
0.1	*A* *B*	0.1766 0.1392	0.1575 0.1473	0.1521 0.1495	0.1509 0.1502	0.1499
0.15	*A* *B*	0.2039 0.1617	0.1856 0.1738	0.1805 0.1773	0.1792 0.1784	0.1798

(Continued)

h/L \ Mesh type \ Mesh number		2×2	4×4	8×8	16×16	Analytical
0.20	*A* *B*	0.2423 0.1931	0.2243 0.2101	0.2191 0.2152	0.2177 0.2167	0.2167
0.25	*A* *B*	0.2918 0.2335	0.2735 0.2561	0.2680 0.2630	0.2664 0.2650	0.2675
0.30	*A* *B*	0.3526 0.2827	0.3333 0.3119	0.3271 0.3210	0.3253 0.3236	0.3227
0.35	*A* *B*	0.4246 0.3409	0.4037 0.3776	0.3967 0.3890	0.3945 0.3924	0.3951

Table 8.5 The central moment of simply-supported square plates subjected to uniform load $q\Big/\left(\dfrac{qL^2}{10}\right)$

h/L \ Mesh type \ Mesh number		2×2	4×4	8×8	16×16	Analytical
10^{-30}	*A* *B*	0.5156 0.4837	0.4885 0.4819	0.4811 0.4799	0.4794 0.4792	0.4789
0.001	*A* *B*	0.5156 0.4837	0.4885 0.4819	0.4811 0.4799	0.4794 0.4792	
0.01	*A* *B*	0.5158 0.4836	0.4887 0.4817	0.4813 0.4797	0.4796 0.4790	
0.1	*A* *B*	0.5296 0.4765	0.4977 0.4775	0.4849 0.4781	0.4806 0.4786	
0.15	*A* *B*	0.5402 0.4722	0.5007 0.4766	0.4854 0.4781	0.4806 0.4786	
0.20	*A* *B*	0.5487 0.4689	0.5023 0.4760	0.4855 0.4780	0.4807 0.4786	
0.25	*A* *B*	0.5548 0.4664	0.5032 0.4757	0.4856 0.4780	0.4807 0.4786	
0.30	*A* *B*	0.5590 0.4646	0.5038 0.4754	0.4857 0.4780	0.4807 0.4786	
0.35	*A* *B*	0.5620 0.4632	0.5041 0.4753	0.4857 0.4780	0.4807 0.4786	

Example 8.2 The central deflection and moment of simply-supported (soft) and clamped circular plates with different thickness-radius ratios (*h/R*) subjected to uniform load.

Assume that the radius of the circular plate is R, the Young's modulus $E = 10.92$, the Poisson's ratio $\mu = 0.3$. Meshes A and B in Fig. 6.14 are used. The results by the element TMT are listed in Tables 8.6 to 8.8.

Table 8.6 The central deflection of simply-supported circular plates subjected to uniform load $q\Big/\left(\dfrac{qR^4}{D}\right)$

h/R \ Mesh	A 24 elements	B 96 elements	Analytical solution
10^{-30}	0.063 033 (−1.05%)	0.063 543 (−0.25%)	0.063 702
0.001	0.063 033 (−1.05%)	0.063 543 (−0.25%)	0.063 702
0.01	0.063 039 (−1.05%)	0.063 549 (−0.25%)	0.063 709
0.1	0.063 689 (−1.13%)	0.064 226 (−0.29%)	0.064 416
0.15	0.064 540 (−1.18%)	0.065 109 (−0.31%)	0.065 309
0.20	0.065 754 (−1.21%)	0.066 353 (−0.31%)	0.066 559
0.25	0.067 330 (−1.23%)	0.067 956 (−0.31%)	0.068 166
0.30	0.069 265 (−1.23%)	0.069 917 (−0.30%)	0.070 130
0.35	0.071 557 (−1.24%)	0.072 235 (−0.30%)	0.072 452

Table 8.7 The central deflection of clamped circular plates subjected to uniform load $q\Big/\left(\dfrac{qR^4}{D}\right)$

h/R \ Mesh	A 24 elements	B 96 elements	Analytical solution
10^{-30}	0.015 954 (2.11%)	0.015 722 (0.62%)	0.015 625
0.001	0.015 954 (2.11%)	0.015 723 (0.63%)	0.015 625
0.01	0.015 960 (2.10%)	0.157 29 (0.62%)	0.015 632
0.1	0.016 618 (1.71%)	0.016 408 (0.42%)	0.016 339
0.15	0.017 476 (1.42%)	0.017 292 (0.35%)	0.017 232
0.20	0.018 697 (1.16%)	0.018 537 (0.30%)	0.018 482
0.25	0.020 278 (0.94%)	0.020 141 (0.26%)	0.020 089
0.30	0.022 217 (0.74%)	0.022 102 (0.22%)	0.022 054
0.35	0.024 513 (0.57%)	0.024 420 (0.18%)	0.024 375

Table 8.8 The central moment of simply-supported circular plates subjected to uniform load $q/\left(qR^2\right)$

Mesh / h/R	A 24 elements	B 96 elements	Analytical solution
10^{-30}	0.209 51 (1.58%)	0.207 54 (0.63%)	0.206 25
0.001	0.209 51 (1.58%)	0.207 54 (0.63%)	
0.01	0.209 52 (1.59%)	0.207 55 (0.63%)	
0.1	0.210 11 (1.87%)	0.207 84 (0.77%)	
0.15	0.210 52 (2.07%)	0.207 93 (0.81%)	
0.20	0.210 82 (2.22%)	0.207 97 (0.83%)	
0.25	0.211 04 (2.32%)	0.207 99 (0.84%)	
0.30	0.211 19 (2.40%)	0.208 01 (0.85%)	
0.35	0.211 30 (2.45%)	0.208 02 (0.86%)	

The above numerical examples show that the element TMT possesses good performance. It has high precision for both deflection and moment, and for both thick and thin plates. And, no shear locking happens.

The scheme starting with assuming ($\boldsymbol{\psi}$, $\boldsymbol{\gamma}$) proposed in this section is a universal method, it can be generalized to construct similar quadrilateral elements[9]. Furthermore, Element DKT, which is formulated by the discrete Kirchhoff theory, is a special case of the present element TMT.

8.6 Generalized Conforming Thick/Thin Plate Elements (2) —Starting with Assuming (w, $\boldsymbol{\gamma}$)

Schemes starting with assuming (w, $\boldsymbol{\gamma}$) for the construction of triangular and quadrilateral thick/thin plate elements have been proposed in references [10] and [11], respectively. This section will introduce the construction procedure of the triangular element TCGC-T9 in [10]. (By the way, another triangular thick/thin element TSL-T9[13] based on the SemiLoof scheme will also be introduced in Sect. 11.5.3).

Main procedure: The variation functions of deflection $\tilde{w}$ and shear strain γ_s long each side of the element are firstly determined using the Timoshenko beam theory. Secondly, the nodal shear strains γ_{xi} and γ_{yi} and the interpolation formulas of the shear strain fields γ_x and γ_y in the domain of the element are then determined according to the shear strain γ_s along each side. Thirdly, assume that the element deflection w is a polynomial containing 9 unknown coefficients $\boldsymbol{\lambda}$. In order to determine λ, 9 generalized conforming conditions (3 point conforming conditions for deflections at the corner nodes, average line conforming conditions for deflections and normal slopes along 3 element sides) are applied. Finally, the rotation and curvature fields are determined from the deflection and shear strain fields; and the element stiffness matrix is then determined by the curvature and shear strain fields. This new element is denoted by TCGC-T9.

When the thickness becomes small, the element TCGC-T9 will automatically degenerate to be the thin plate element GPL-T9 in reference [14]. So, no shear locking will happen.

Consider the triangular thick plate element shown in Fig. 8.11. The element nodal displacement vector is formed by 9 engineering DOFs:

$$\boldsymbol{q}^e = [w_1 \quad \psi_{x1} \quad \psi_{y1} \quad w_2 \quad \psi_{x2} \quad \psi_{y2} \quad w_3 \quad \psi_{x3} \quad \psi_{y3}]^{\mathrm{T}}$$

8.6.1 Boundary Displacements of the Element

On the element boundary, the deflection $\tilde{w}$ is assumed according to the thick beam theory, and the normal slope $\tilde{\psi}_n$ is assumed to be a linear function. For example, along the element side $\overline{12}$, we have

$$\left.\begin{aligned}
\tilde{w}_{12} &= [L_1 + \mu_{e3}L_1L_2(L_1 - L_2)]w_1 + \frac{1}{2}L_1L_2[1 + \mu_{e3}(L_1 - L_2)](c_3\psi_{x1} - b_3\psi_{y1}) \\
&\quad + [L_2 - \mu_{e3}L_1L_2(L_1 - L_2)]w_2 + \frac{1}{2}L_1L_2[-1 + \mu_{e3}(L_1 - L_2)](c_3\psi_{x2} - b_3\psi_{y2}) \\
\tilde{\psi}_n &= -\frac{L_1}{d_3}(b_3\psi_{x1} + c_3\psi_{y1}) - \frac{L_2}{d_3}(b_3\psi_{x2} + c_3\psi_{y2})
\end{aligned}\right\} \tag{8-146}$$

where

$$\mu_{ei} = 1 - 2\delta_i \quad (i = 1,2,3)$$

δ_i is given by Eq. (8-114).

8.6.2 Shear Strain Fields of the Element

Firstly, the shear strain γ_s along each side is determined from the thick beam theory; Then, the shear strains γ_{xi} and γ_{yi} at the corner node i are determined; finally, the interpolation formulas for shear strains γ_x and γ_y in the domain of the element can be obtained. The above derivation procedure has been given in Sect. 8.5.

Formulas in Eq. (8-138) are the interpolation formulas of element shear strains.

8.6.3 Deflection Field of the Element

1. Displacements in the domain of the element

The element deflection field is assumed as

$$w = \boldsymbol{F}_\lambda \boldsymbol{\lambda} \tag{8-147}$$

where

$$\boldsymbol{\lambda} = [\lambda_1 \quad \lambda_2 \quad \lambda_3 \quad \lambda_4 \quad \lambda_5 \quad \lambda_6 \quad \lambda_7 \quad \lambda_8 \quad \lambda_9]^{\mathrm{T}}$$

$$\begin{aligned}\boldsymbol{F}_\lambda = [&L_1 \quad L_2 \quad L_3 \quad L_1L_2 \quad L_2L_3 \quad L_3L_1 \\ &L_1\left(L_1-\frac{1}{2}\right)(L_1-1) \quad L_2\left(L_2-\frac{1}{2}\right)(L_2-1) \quad L_3\left(L_3-\frac{1}{2}\right)(L_3-1)]\end{aligned} \tag{8-148}$$

Then, the element rotation fields can be obtained as

$$\begin{Bmatrix} \psi_x \\ \psi_y \end{Bmatrix} = \begin{Bmatrix} \dfrac{\partial w}{\partial x} - \gamma_x \\ \dfrac{\partial w}{\partial y} - \gamma_y \end{Bmatrix} \tag{8-149}$$

2. Introducing generalized conforming conditions

The same line-point conforming scheme as that of the thin plate element GPL-T9 is used:

$$\left.\begin{aligned} &w_i - \tilde{w}_i = 0 \\ &\int_{d_i} (w - \tilde{w})\mathrm{d}s = 0 \\ &\int_{d_i} (\psi_n - \tilde{\psi}_n)\mathrm{d}s = 0 \end{aligned}\right\} \quad (i = 1,2,3) \tag{8-150}$$

Substitution of Eqs. (8-146) and (8-147) into the above equation yields

$$\boldsymbol{\lambda} = \hat{\boldsymbol{A}}\boldsymbol{q}^e \tag{8-151}$$

where

$$\hat{\boldsymbol{A}}=\left[\begin{array}{ccccccccc}1 & 0 & 0 & 0 & 0 & 0 & 0 & 0 & 0\\ 0 & 0 & 0 & 1 & 0 & 0 & 0 & 0 & 0\\ 0 & 0 & 0 & 0 & 0 & 0 & 1 & 0 & 0\\ 0 & \frac{1}{2}c_3 & -\frac{1}{2}b_3 & 0 & -\frac{1}{2}c_3 & \frac{1}{2}b_3 & 0 & 0 & 0\\ 0 & 0 & 0 & 0 & \frac{1}{2}c_1 & -\frac{1}{2}b_1 & 0 & -\frac{1}{2}c_1 & \frac{1}{2}b_1\\ 0 & -\frac{1}{2}c_2 & \frac{1}{2}b_2 & 0 & 0 & 0 & 0 & \frac{1}{2}c_2 & -\frac{1}{2}b_2\\ & \hat{\boldsymbol{A}}_1 & & & \hat{\boldsymbol{A}}_2 & & & \hat{\boldsymbol{A}}_3 & \end{array}\right] \tag{8-152}$$

$$\hat{\boldsymbol{A}}_1=\begin{bmatrix}-(\mu_{e2}+\mu_{e3}) & \frac{1}{2}(c_2\mu_{e2}-c_3\mu_{e3}) & -\frac{1}{2}(b_2\mu_{e2}-b_3\mu_{e3})\\ \mu_{e3}-r_2\mu_{e2} & \frac{1}{2}(r_2c_2\mu_{e2}+c_3\mu_{e3}) & -\frac{1}{2}(r_2b_2\mu_{e2}+b_3\mu_{e3})\\ \mu_{e2}+r_3\mu_{e3} & \frac{1}{2}(r_3c_3\mu_{e3}-c_2\mu_{e2}) & -\frac{1}{2}(r_3b_3\mu_{e3}-b_2\mu_{e2})\end{bmatrix} \tag{8-153a}$$

$$\hat{\boldsymbol{A}}_2=\begin{bmatrix}\mu_{e3}+r_1\mu_{e1} & \frac{1}{2}(r_1c_1\mu_{e1}-c_3\mu_{e3}) & -\frac{1}{2}(r_1b_1\mu_{e1}-b_3\mu_{e3})\\ -(\mu_{e3}+\mu_{e1}) & \frac{1}{2}(c_3\mu_{e3}-c_1\mu_{e1}) & -\frac{1}{2}(b_3\mu_{e3}-b_1\mu_{e1})\\ \mu_{e1}-r_3\mu_{e3} & \frac{1}{2}(r_3c_3\mu_{e3}+c_1\mu_{e1}) & -\frac{1}{2}(r_3b_3\mu_{e3}+b_1\mu_{e1})\end{bmatrix} \tag{8-153b}$$

$$\hat{\boldsymbol{A}}_3=\begin{bmatrix}\mu_{e2}-r_1\mu_{e1} & \frac{1}{2}(r_1c_1\mu_{e1}+c_2\mu_{e2}) & -\frac{1}{2}(r_1b_1\mu_{e1}+b_2\mu_{e2})\\ \mu_{e1}+r_2\mu_{e2} & \frac{1}{2}(r_2c_2\mu_{e2}-c_1\mu_{e1}) & -\frac{1}{2}(r_2b_2\mu_{e2}-b_1\mu_{e1})\\ -(\mu_{e1}+\mu_{e2}) & \frac{1}{2}(c_1\mu_{e1}-c_2\mu_{e2}) & -\frac{1}{2}(b_1\mu_{e1}-b_2\mu_{e2})\end{bmatrix} \tag{8-153c}$$

$$r_1=\frac{d_2^2-d_3^2}{d_1^2},\quad r_2=\frac{d_3^2-d_1^2}{d_2^2},\quad r_3=\frac{d_1^2-d_2^2}{d_3^2} \tag{8-154}$$

Substitution of Eq. (8-151) into Eq. (8-147) yields

$$w=\boldsymbol{N}\boldsymbol{q}^e$$

where

$$\boldsymbol{N} = [N_{w1} \quad N_{\psi x1} \quad N_{\psi y1} \quad N_{w2} \quad N_{\psi x2} \quad N_{\psi y2} \quad N_{w3} \quad N_{\psi x3} \quad N_{\psi y3}] \tag{8-155}$$

$$\left.\begin{aligned}
N_{wi} &= L_i - (\mu_{ej} + \mu_{em})L_i\left(L_i - \frac{1}{2}\right)(L_i - 1) + (\mu_{em} - r_j\mu_{ej})L_j\left(L_j - \frac{1}{2}\right)(L_j - 1) \\
&\quad + (\mu_{ej} + r_m\mu_{em})L_m\left(L_m - \frac{1}{2}\right)(L_m - 1) \\
N_{\psi xi} &= \frac{1}{2}\left[L_i(c_m L_j - c_j L_m) + (c_j\mu_{ej} - c_m\mu_{em})L_i\left(L_i - \frac{1}{2}\right)(L_i - 1)\right. \\
&\quad + (r_j c_j \mu_{ej} + c_m\mu_{em})L_j\left(L_j - \frac{1}{2}\right)(L_j - 1) \\
&\quad \left. + (r_m c_m \mu_{em} - c_j\mu_{ej})L_m\left(L_m - \frac{1}{2}\right)(L_m - 1)\right] \\
N_{\psi yi} &= \frac{1}{2}\left[L_i(-b_m L_j + b_j L_m) - (b_j\mu_{ej} - b_m\mu_{em})L_i\left(L_i - \frac{1}{2}\right)(L_i - 1)\right. \\
&\quad - (r_j b_j \mu_{ej} + b_m\mu_{em})L_j\left(L_j - \frac{1}{2}\right)(L_j - 1) \\
&\quad \left. - (r_m b_m \mu_{em} - b_j\mu_{ej})L_m\left(L_m - \frac{1}{2}\right)(L_m - 1)\right] \quad (\overrightarrow{\underleftarrow{i, j, m}} = \overrightarrow{\underleftarrow{1,2,3}})
\end{aligned}\right\} \tag{8-156}$$

8.6.4 Stiffness Matrix of the Element

1. The element bending strain matrix

The element curvature fields are

$$\boldsymbol{\kappa} = [\kappa_x \quad \kappa_y \quad 2\kappa_{xy}]^{\mathrm{T}} = \left[-\frac{\partial \psi_x}{\partial x} \quad -\frac{\partial \psi_y}{\partial y} \quad -\left(\frac{\partial \psi_x}{\partial y} + \frac{\partial \psi_y}{\partial x}\right)\right]^{\mathrm{T}} \tag{8-157}$$

Substitution of Eq. (8-149) into the above equation yields

$$\boldsymbol{\kappa} = \left[-\frac{\partial^2 w}{\partial x^2} + \frac{\partial \gamma_x}{\partial x} \quad -\frac{\partial^2 w}{\partial y^2} + \frac{\partial \gamma_y}{\partial y} \quad -2\frac{\partial^2 w}{\partial x \partial y} + \frac{\partial \gamma_x}{\partial y} + \frac{\partial \gamma_y}{\partial x}\right]^{\mathrm{T}}$$

From Eq. (8-140), we have

$$\frac{\partial \gamma_x}{\partial x} = 0, \quad \frac{\partial \gamma_y}{\partial y} = 0, \quad \frac{\partial \gamma_x}{\partial y} + \frac{\partial \gamma_y}{\partial x} = 0$$

So, we obtain

$$\boldsymbol{\kappa} = \left[-\frac{\partial^2 w}{\partial x^2} \quad -\frac{\partial^2 w}{\partial y^2} \quad -2\frac{\partial^2 w}{\partial x \partial y} \right]^{\mathrm{T}} = \boldsymbol{B}_{\mathrm{b}} \boldsymbol{q}^e \tag{8-158}$$

where $\boldsymbol{B}_{\mathrm{b}}$ is the element bending strain matrix

$$\boldsymbol{B}_{\mathrm{b}} = \left[\boldsymbol{B}_{\mathrm{b}1} \quad \boldsymbol{B}_{\mathrm{b}2} \quad \boldsymbol{B}_{\mathrm{b}3} \right] \tag{8-159}$$

$$\boldsymbol{B}_{\mathrm{b}i} = \begin{bmatrix} B_{\mathrm{b}i11} & B_{\mathrm{b}i12} & B_{\mathrm{b}i13} \\ B_{\mathrm{b}i21} & B_{\mathrm{b}i22} & B_{\mathrm{b}i23} \\ B_{\mathrm{b}i31} & B_{\mathrm{b}i32} & B_{\mathrm{b}i33} \end{bmatrix} \quad (i = 1,2,3) \tag{8-160}$$

$$\begin{aligned}
B_{\mathrm{b}i11} = & -\frac{3}{4A^2}[-b_i^2(\mu_{ej} + \mu_{em})(2L_i - 1) + b_j^2(\mu_{em} - r_j\mu_{ej})(2L_j - 1) \\
& + b_m^2(\mu_{ej} + r_m\mu_{em})(2L_m - 1)] \\
B_{\mathrm{b}i21} = & -\frac{3}{4A^2}[-c_i^2(\mu_{ej} + \mu_{em})(2L_i - 1) + c_j^2(\mu_{em} - r_j\mu_{ej})(2L_j - 1) \\
& + c_m^2(\mu_{ej} + r_m\mu_{em})(2L_m - 1)] \\
B_{\mathrm{b}i31} = & -\frac{3}{2A^2}[-b_ic_i(\mu_{ej} + \mu_{em})(2L_i - 1) + b_jc_j(\mu_{em} - r_j\mu_{ej})(2L_j - 1) \\
& + b_mc_m(\mu_{ej} + r_m\mu_{em})(2L_m - 1)] \\
B_{\mathrm{b}i12} = & -\frac{3}{8A^2}[b_i^2(c_j\mu_{ej} - c_m\mu_{em})(2L_i - 1) + b_j^2(r_jc_j\mu_{ej} + c_m\mu_{em})(2L_j - 1) \\
& + b_m^2(r_mc_m\mu_{em} - c_j\mu_{ej})(2L_m - 1) + \frac{2}{3}b_i(b_jc_m - b_mc_j)] \\
B_{\mathrm{b}i22} = & -\frac{3}{8A^2}[c_i^2(c_j\mu_{ej} - c_m\mu_{em})(2L_i - 1) + c_j^2(r_jc_j\mu_{ej} + c_m\mu_{em})(2L_j - 1) \\
& + c_m^2(r_mc_m\mu_{em} - c_j\mu_{ej})(2L_m - 1)] \\
B_{\mathrm{b}i32} = & -\frac{3}{4A^2}[b_ic_i(c_j\mu_{ej} - c_m\mu_{em})(2L_i - 1) + b_jc_j(r_jc_j\mu_{ej} + c_m\mu_{em})(2L_j - 1) \\
& + b_mc_m(r_mc_m\mu_{em} - c_j\mu_{ej})(2L_m - 1) + \frac{1}{3}c_i(b_jc_m - b_mc_j)] \\
B_{\mathrm{b}i13} = & -\frac{3}{8A^2}[b_i^2(b_m\mu_{em} - b_j\mu_{ej})(2L_i - 1) - b_j^2(r_jb_j\mu_{ej} + b_m\mu_{em})(2L_j - 1) \\
& - b_m^2(r_mb_m\mu_{em} - b_j\mu_{ej})(2L_m - 1)] \\
B_{\mathrm{b}i23} = & -\frac{3}{8A^2}[c_i^2(b_m\mu_{em} - b_j\mu_{ej})(2L_i - 1) - c_j^2(r_jb_j\mu_{ej} + b_m\mu_{em})(2L_j - 1) \\
& - c_m^2(r_mb_m\mu_{em} - b_j\mu_{ej})(2L_m - 1) + \frac{2}{3}c_i(b_jc_m - b_mc_j)]
\end{aligned}$$

$$B_{\mathrm{b}i33}=-\frac{3}{4A^2}[b_ic_i(b_m\mu_{em}-b_j\mu_{ej})(2L_i-1)-b_jc_j(r_jb_j\mu_{ej}+b_m\mu_{em})(2L_j-1)$$
$$-b_mc_m(r_mb_m\mu_{em}-b_j\mu_{ej})(2L_m-1)+\frac{1}{3}b_i(b_jc_m-b_mc_j)]\quad(\overleftrightarrow{i,j,m}=\overleftrightarrow{1,2,3})$$

2. The element shear strain matrix

The element shear strain matrix is given by Eq. (8-139)

$$\boldsymbol{B}_{\mathrm{s}}=\begin{bmatrix}\boldsymbol{B}_{\mathrm{s}1} & \boldsymbol{B}_{\mathrm{s}2} & \boldsymbol{B}_{\mathrm{s}3}\end{bmatrix} \tag{8-161}$$

where

$$\boldsymbol{B}_{\mathrm{s}i}=\frac{1}{2A}\begin{bmatrix}2\delta_j(b_iL_m-b_mL_i)-2\delta_m(b_jL_i-b_iL_j) & -c_j\delta_j(b_iL_m-b_mL_i)-c_m\delta_m(b_jL_i-b_iL_j) & b_j\delta_j(b_iL_m-b_mL_i)+b_m\delta_m(b_jL_i-b_iL_j)\\ 2\delta_j(c_iL_m-c_mL_i)-2\delta_m(c_jL_i-c_iL_j) & -c_j\delta_j(c_iL_m-c_mL_i)-c_m\delta_m(c_jL_i-c_iL_j) & b_j\delta_j(c_iL_m-c_mL_i)+b_m\delta_m(c_jL_i-c_iL_j)\end{bmatrix}\quad(i,j,m=\overleftrightarrow{1,2,3}) \tag{8-162}$$

3. The element stiffness matrix

The element stiffness matrix is

$$\boldsymbol{K}^e=\begin{bmatrix}\boldsymbol{K}_{11} & \boldsymbol{K}_{12} & \boldsymbol{K}_{13}\\ \boldsymbol{K}_{21} & \boldsymbol{K}_{22} & \boldsymbol{K}_{23}\\ \boldsymbol{K}_{31} & \boldsymbol{K}_{32} & \boldsymbol{K}_{33}\end{bmatrix} \tag{8-163}$$

where
$$\boldsymbol{K}_{ij}=\iint_{A^e}\boldsymbol{B}_{\mathrm{b}i}^{\mathrm{T}}\boldsymbol{D}_{\mathrm{b}}\boldsymbol{B}_{\mathrm{b}j}\mathrm{d}A+\iint_{A^e}\boldsymbol{B}_{\mathrm{s}i}^{\mathrm{T}}\boldsymbol{D}_{\mathrm{s}}\boldsymbol{B}_{\mathrm{s}j}\mathrm{d}A\quad(i,j=1,2,3) \tag{8-164}$$

$$\boldsymbol{D}_{\mathrm{b}}=D\begin{bmatrix}1 & \mu & 0\\ \mu & 1 & 0\\ 0 & 0 & \dfrac{1-\mu}{2}\end{bmatrix},\quad \boldsymbol{D}_{\mathrm{s}}=C\begin{bmatrix}1 & 0\\ 0 & 1\end{bmatrix}$$

$$D=\frac{Eh^3}{12(1-\mu^2)},\quad C=\frac{5}{6}Gh=\frac{5D(1-\mu)}{h^2}$$

E is the Young's modulus; G is the shear modulus.

8.6.5 Numerical Examples

Example 8.3 The central deflection and moment of simply-supported (hard) square plates (the side length is L) subjected to uniform load.

Meshes A and B in Fig. 8.12 are still adopted, $\mu = 0.3$. The results by the element TCGC-T9 are given in Tables 8.9 to 8.11.

Table 8.9 The central deflection of simply-supported square plates subjected to uniform load $q\Big/\left(\dfrac{qL^4}{100D}\right)$

h/L \ Mesh number / Mesh type		2×2	4×4	8×8	16×16	Analytical
10^{-30}	*A*	0.3803	0.4007	0.4050	0.4059	0.4062
	B	0.3948	0.4038	0.4057	0.4061	
0.001	*A*	0.3803	0.4007	0.4050	0.4059	0.4062
	B	0.3948	0.4038	0.4057	0.4061	
0.01	*A*	0.3804	0.4008	0.4051	0.4061	0.4064
	B	0.3950	0.4039	0.4058	0.4062	
0.1	*A*	0.3978	0.4183	0.4244	0.4265	0.4273
	B	0.4079	0.4194	0.4243	0.4264	
0.15	*A*	0.4214	0.4434	0.4506	0.4528	0.4536
	B	0.4254	0.4424	0.4500	0.4526	
0.20	*A*	0.4562	0.4799	0.4876	0.4897	0.4906
	B	0.4519	0.4763	0.4862	0.4893	
0.25	*A*	0.5025	0.5276	0.5352	0.5372	0.5379
	B	0.4880	0.5207	0.5328	0.5364	
0.30	*A*	0.5606	0.5863	0.5935	0.5952	0.5956
	B	0.5338	0.5754	0.5899	0.5941	
0.35	*A*	0.6304	0.6559	0.6624	0.6638	0.6641
	B	0.5892	0.6402	0.6573	0.6622	

Table 8.10 The central deflection of clamped square plates subjected to uniform load $q\Big/\left(\dfrac{qL^4}{100D}\right)$

h/L \ Mesh number / Mesh type		2×2	4×4	8×8	16×16	Analytical
10^{-30}	*A*	0.1167	0.1241	0.1261	0.1265	0.1265
	B	0.0997	0.1192	0.1247	0.1260	

(Continued)

h/L \ Mesh number / Mesh type		2×2	4×4	8×8	16×16	Analytical
0.001	*A*	0.1167	0.1241	0.1261	0.1265	0.1265
	B	0.0997	0.1192	0.1247	0.1260	
0.01	*A*	0.1169	0.1242	0.1263	0.1266	0.1265
	B	0.0998	0.1194	0.1249	0.1262	
0.1	*A*	0.1363	0.1440	0.1477	0.1496	0.1499
	B	0.1131	0.1376	0.1462	0.1492	
0.15	*A*	0.1604	0.1704	0.1758	0.1779	0.1798
	B	0.1310	0.1623	0.1737	0.1774	
0.20	*A*	0.1948	0.2080	0.2144	0.2165	0.2167
	B	0.1579	0.1975	0.2115	0.2157	
0.25	*A*	0.2403	0.2565	0.2632	0.2652	0.2675
	B	0.1942	0.2427	0.2593	0.2641	
0.30	*A*	0.2974	0.3158	0.3224	0.3241	0.3227
	B	0.2401	0.2980	0.3172	0.3226	
0.35	*A*	0.3662	0.3858	0.3919	0.3933	0.3951
	B	0.2956	0.3634	0.3852	0.3914	

Table 8.11 The central moment of simply-supported square plates subjected to uniform load $q\Big/\left(\dfrac{qL^2}{10}\right)$

h/L \ Mesh number / Mesh type		2×2	4×4	8×8	16×16	Analytical
10^{-30}	*A*	0.4928	0.4768	0.4771	0.4781	
	B	0.5024	0.4878	0.4823	0.4800	
0.001	*A*	0.4928	0.4768	0.4771	0.4781	
	B	0.5024	0.4878	0.4823	0.4800	
0.01	*A*	0.4932	0.4776	0.4780	0.4789	
	B	0.5026	0.4880	0.4824	0.4800	
0.1	*A*	0.5238	0.4986	0.4858	0.4809	0.4789
	B	0.5193	0.4987	0.4867	0.4814	
0.15	*A*	0.5435	0.5048	0.4870	0.4810	
	B	0.5329	0.5039	0.4877	0.4815	
0.20	*A*	0.5600	0.5090	0.4876	0.4811	
	B	0.5453	0.5073	0.4882	0.4815	

(Continued)

h/L \ Mesh number / Mesh type		2×2	4×4	8×8	16×16	Analytical
0.25	*A*	0.5736	0.5118	0.4880	0.4811	0.4789
	B	0.5557	0.5094	0.4884	0.4815	
0.30	*A*	0.5849	0.5138	0.4881	0.4811	
	B	0.5639	0.5107	0.4885	0.4816	
0.35	*A*	0.5941	0.5152	0.4883	0.4811	
	B	0.5704	0.5116	0.4886	0.4816	

Example 8.4 The central deflection and moment of simply-supported (soft) and clamped circular plates subjected to uniform load.

The two meshes (*A* and *B*) shown in Fig. 6.14 are still adopted. Assume that $E = 10.92$, $\mu = 0.3$. The results by the element TCGC-T9 are given in Tables 8.12 to 8.14.

The above numerical examples show that the element TCGC-T9 also possesses good performance. It has high precision for both deflection and moment, and for both thick and thin plates. And, no shear locking happens.

By the comparison of the elements TCGC-T9 and TMT, we can conclude that,

(1) The precisions of these two elements belong to the same magnitude.

(2) For relatively thin plates, the element TCGC-T9 is a little better than the element TMT. This is because for the very thin plate cases, the elements TCGC-T9 and TMT will degenerate to be the thin plate elements GPL-T9 and DKT, respectively. Note that the element GPL-T9 is a little better than the element DKT.

Table 8.12 The central deflection of simply-supported circular plates subjected to uniform load $q\Big/\left(\dfrac{qR^4}{D}\right)$

h/R \ Mesh	*A* 24 elements	*B* 96 elements	Analytical
10^{-30}	0.063 818 (0.18%)	0.063 728 (0.04%)	0.063 702
0.001	0.063 818 (0.18%)	0.063 728 (0.04%)	0.063 702
0.01	0.063 821 (0.18%)	0.063 731 (0.03%)	0.063 709
0.1	0.064 242 (−0.27%)	0.064 247 (−0.26%)	0.064 416
0.15	0.064 901 (−0.62%)	0.065 043 (−0.41%)	0.065 309
0.20	0.065 921 (−0.96%)	0.066 222 (−0.51%)	0.066 559
0.25	0.067 315 (−1.25%)	0.067 777 (−0.57%)	0.068 166
0.30	0.069 088 (−1.49%)	0.069 704 (−0.61%)	0.070 130
0.35	0.071 241 (−1.67%)	0.071 998 (−0.63%)	0.072 452

Table 8.13 The central deflection of clamped circular plates subjected to uniform load $q\Big/\left(\dfrac{qR^4}{D}\right)$

Mesh / h/R	A 24 elements	B 96 elements	Analytical
10^{-30}	0.014 515 (−7.10%)	0.015 342 (−1.81%)	0.015 625
0.001	0.014 515 (−7.10%)	0.015 342 (−1.81%)	0.015 625
0.01	0.014 518 (−7.13%)	0.015 345 (−1.84%)	0.015 632
0.1	0.014 938 (−8.57%)	0.015 861 (−2.93%)	0.016 339
0.15	0.015 595 (−9.50%)	0.016 657 (−3.34%)	0.017 232
0.20	0.016 613 (−10.11%)	0.017 836 (−3.50%)	0.018 482
0.25	0.018 007 (−10.36%)	0.019 392 (−3.47%)	0.020 089
0.30	0.019 782 (−10.30%)	0.021 319 (−3.33%)	0.022 054
0.35	0.021 936 (−10.01%)	0.023 613 (−3.13%)	0.024 375

Table 8.14 The central moment of simply-supported circular plates subjected to uniform load $q\big/\left(qR^2\right)$

Mesh / h/R	A 24 elements	B 96 elements	Analytical
10^{-11}	0.210 28 (1.95%)	0.207 36 (0.54%)	0.206 25
0.001	0.210 28 (1.95%)	0.207 36 (0.54%)	
0.01	0.210 29 (1.96%)	0.207 37 (0.54%)	
0.1	0.211 40 (2.50%)	0.208 15 (0.92%)	
0.15	0.212 42 (2.99%)	0.208 49 (1.09%)	
0.20	0.213 35 (3.44%)	0.208 69 (1.18%)	
0.25	0.214 11 (3.81%)	0.208 82 (1.25%)	
0.30	0.214 70 (4.10%)	0.208 91 (1.29%)	
0.35	0.215 16 (4.32%)	0.208 96 (1.31%)	

(3) For relatively thick plates, the element TMT is a little better than the element TCGC-T9. This is because the shear strain fields of these two elements are the same, only curvature fields are different; the rotation fields of the element TMT are assumed directly, only first-order differential operation is needed when we determine the curvature fields by such rotation fields, so the accuracy loss is relatively less; but in the element TCGC-T9, the deflection field is assumed directly, second-order differential operation must be performed when we determine the curvature fields by such deflection field, so the accuracy loss is relatively more.

(4) When we determine the element equivalent nodal load vector due to transverse distributed load, the element TCGC-T9 is more convenient. This is because the shape functions for the deflection of the element TCGC-T9 have

already been given, so the equivalent nodal load vector can be determined from these shape functions directly; but the deflection field of the element TMT is undetermined, so, before deriving the element equivalent nodal load vector, supplementary work, assumption of rational interpolation formula for deflection field, is needed.

8.7 Generalized Conforming Thin/Thick Plate Elements —From Thin to Thick Plate Elements

By starting with a thin plate element and introducing shear deformation, the thin plate element can be generalized to a new thin/thick plate element. Such transition schemes have been studied in references [15−19].

In 1986, Fricker[15] proposed a simple method for including shear deformation in the thin plate elements, but the thick plate element he suggested cannot strictly pass the thick plate patch test.

Based on the displacement field of the rectangular thin plate element ACM, reference [16] developed a rectangular thick plate element with 12 DOFs by introducing additional displacement field and linear shear strain fields. The key point is that two generalized conforming conditions are adopted: (1) the conforming conditions for displacements between two adjacent elements; (2) the generalized conforming conditions between shear strains and displacements. The element obtained can pass pure bending, pure twisting and constant shear force patch tests, which provides the first successful experience for the schemes of transition from thin plate elements to thin / thick plate elements.

In reference [17], the displacement fields of the thick plate element were decomposed into two parts: displacement fields for the thin plate element and supplementary displacement fields for the thick plate element. Then, based on the two thin plate elements LR12-2[20] and ACM[21], two new thin/thick plate elements LFR1 and LFR2 were constructed. Now, their construction procedure will be introduced as follows.

8.7.1 Decomposition of the Displacement Fields of the Rectangular Thick Plate Element

Consider a rectangular thick plate element shown in Fig. 8.13. Its nodal displacement vector is composed of 12 DOFs

$$\boldsymbol{q}^e = [w_1 \quad \psi_{x1} \quad \psi_{y1} \quad w_2 \quad \psi_{x2} \quad \psi_{y2} \quad w_3 \quad \psi_{x3} \quad \psi_{y3} \quad w_4 \quad \psi_{x4} \quad \psi_{y4}]^{\mathrm{T}}$$

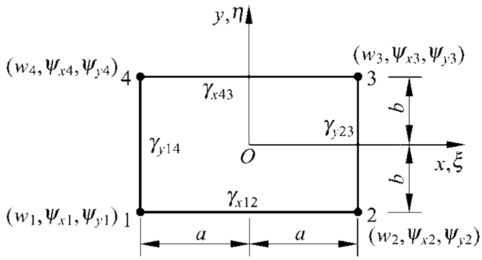

Figure 8.13 Rectangular thick plate element

The displacement fields in the domain of the element are assumed as

$$\left.\begin{aligned} w &= w^0 + w^* \\ \psi_x &= \psi_x^0 + \psi_x^* = \frac{\partial w^0}{\partial x} + \psi_x^* \\ \psi_y &= \psi_y^0 + \psi_y^* = \frac{\partial w^0}{\partial y} + \psi_y^* \end{aligned}\right\} \tag{8-165}$$

where w, ψ_x, ψ_y denote the displacements of the thick plate element; w^0, ψ_x^0, ψ_y^0 denote the displacements of a thin plate element that can be used; and w^*, ψ_x^*, ψ_y^* denote the supplementary displacements of the thick plate element.

The boundary displacements of the thick plate element are assumed as

$$\left.\begin{aligned} \tilde{w} &= \tilde{w}^0 + \tilde{w}^* \\ \tilde{\psi}_s &= \tilde{\psi}_s^0 + \tilde{\psi}_s^* \\ \tilde{\psi}_n &= \tilde{\psi}_n^0 + \tilde{\psi}_n^* \end{aligned}\right\} \tag{8-166}$$

in which n and s denote the normal and tangential directions of the boundary, respectively.

8.7.2 Determination of the Supplementary Displacements of the Thick Plate Element

In order to determine the supplementary displacement fields of the thick plate element, the transverse shear strain γ_s and the supplementary displacements $\tilde{w}^*$, $\tilde{\psi}_s^*$ and $\tilde{\psi}_n^*$ along each element side are firstly determined from the formulas of thick/thin beam; then the supplementary displacements w^*, ψ_x^* and ψ_y^* in the domain of the element are determined.

Firstly, from Eq. (8-99c), the transverse shear strains along each element side are as follows:

$$\left.\begin{aligned}\gamma_{x12} &= -\frac{\delta_1}{a}[w_1 - w_2 + a(\psi_{x1} + \psi_{x2})]\\ \gamma_{x43} &= -\frac{\delta_1}{a}[w_4 - w_3 + a(\psi_{x4} + \psi_{x3})]\\ \gamma_{y23} &= -\frac{\delta_2}{b}[w_2 - w_3 + b(\psi_{y2} + \psi_{y3})]\\ \gamma_{y14} &= -\frac{\delta_2}{b}[w_1 - w_4 + b(\psi_{y1} + \psi_{y4})]\end{aligned}\right\} \tag{8-167}$$

From Eq. (8-100), we obtain

$$\delta_1 = \frac{\left(\frac{h}{a}\right)^2}{\frac{10}{3}(1-\mu) + 2\left(\frac{h}{a}\right)^2}, \quad \delta_2 = \frac{\left(\frac{h}{b}\right)^2}{\frac{10}{3}(1-\mu) + 2\left(\frac{h}{b}\right)^2} \tag{8-168}$$

h is the thickness of the plate; μ is the Poisson's ratio.

Secondly, the supplementary displacements $\tilde{w}^*$, $\tilde{\psi}_s^*$ and $\tilde{\psi}_n^*$ along each element side are determined. From the fundamental formulas of the thick beam element (8-99a,b), $\tilde{w}^*$ and $\tilde{\psi}_s^*$ can be written as

$$\left.\begin{aligned}\tilde{w}^* &= \gamma d t(1-t)(1-2t)\\ \tilde{\psi}_s^* &= -6\gamma t(1-t)\end{aligned}\right\} \tag{8-169}$$

Furthermore, $\tilde{\psi}_n^*$ can be assumed to be zero. Therefore, the supplementary displacements along 4 boundary lines can be obtained as

$$\left.\begin{array}{llll}\text{side 12} & \tilde{w}^* = -\frac{1}{2}\gamma_{x12} a\xi(1-\xi^2), & \tilde{\psi}_x^* = -\frac{3}{2}\gamma_{x12}(1-\xi^2), & \tilde{\psi}_y^* = 0\\ \text{side 23} & \tilde{w}^* = -\frac{1}{2}\gamma_{y23} b\eta(1-\eta^2), & \tilde{\psi}_y^* = -\frac{3}{2}\gamma_{y23}(1-\eta^2), & \tilde{\psi}_x^* = 0\\ \text{side 43} & \tilde{w}^* = -\frac{1}{2}\gamma_{x43} a\xi(1-\xi^2), & \tilde{\psi}_x^* = -\frac{3}{2}\gamma_{x43}(1-\xi^2), & \tilde{\psi}_y^* = 0\\ \text{side 14} & \tilde{w}^* = -\frac{1}{2}\gamma_{y14} b\eta(1-\eta^2), & \tilde{\psi}_y^* = -\frac{3}{2}\gamma_{y14}(1-\eta^2), & \tilde{\psi}_x^* = 0\end{array}\right\} \tag{8-170}$$

where $\xi = \frac{x}{a}$, $\eta = \frac{y}{b}$.

Finally, the supplementary displacements in the domain of the element are determined. According to Eq. (8-170), the interpolation formulas for the supplementary displacement field in the domain of the element can be written as

$$\left.\begin{aligned}
w^* &= -\frac{a}{2}\left[\gamma_{x12}\left(\frac{1-\eta}{2}\right)+\gamma_{x43}\left(\frac{1+\eta}{2}\right)\right]\xi(1-\xi^2)\\
&\quad -\frac{b}{2}\left[\gamma_{y14}\left(\frac{1-\xi}{2}\right)+\gamma_{y23}\left(\frac{1+\xi}{2}\right)\right]\eta(1-\eta^2)\\
\psi_x^* &= -\frac{3}{2}\left[\gamma_{x12}\left(\frac{1-\eta}{2}\right)+\gamma_{x43}\left(\frac{1+\eta}{2}\right)\right](1-\xi^2)\\
\psi_y^* &= -\frac{3}{2}\left[\gamma_{y14}\left(\frac{1-\xi}{2}\right)+\gamma_{y23}\left(\frac{1+\xi}{2}\right)\right](1-\eta^2)
\end{aligned}\right\} \tag{8-171}$$

It can be seen that, the supplementary displacements in the domain of the element given in Eq. (8-171) are exactly compatible with the boundary supplementary displacements given in Eq. (8-170).

Substituting Eq. (8-167) into Eq. (8-171), the supplementary displacements in the domain of the element can be obtained as:

$$\left.\begin{aligned}
w^* &= -\frac{\delta_1}{4}\left[\sum_{i=1}^{4} w_i\xi_i(1+\eta_i\eta)-a\sum_{i=1}^{4}\psi_{xi}(1+\eta_i\eta)\right]\xi(1-\xi^2)\\
&\quad -\frac{\delta_2}{4}\left[\sum_{i=1}^{4} w_i\eta_i(1+\xi_i\xi)-b\sum_{i=1}^{4}\psi_{yi}(1+\xi_i\xi)\right]\eta(1-\eta^2)\\
\psi_x^* &= -\frac{3\delta_1}{4a}\left[\sum_{i=1}^{4} w_i\xi_i(1+\eta_i\eta)-a\sum_{i=1}^{4}\psi_{xi}(1+\eta_i\eta)\right](1-\xi^2)\\
\psi_y^* &= -\frac{3\delta_2}{4b}\left[\sum_{i=1}^{4} w_i\eta_i(1+\xi_i\xi)-b\sum_{i=1}^{4}\psi_{yi}(1+\xi_i\xi)\right](1-\eta^2)
\end{aligned}\right\} \tag{8-172}$$

8.7.3 Two Thin/Thick Plate Elements

Two new universal elements LFR1 and LFR2 for both thick and thin plates are constructed based on two high quality thin plate elements (elements LR12-2 and ACM), respectively. The displacement field w^0 of the thin plate element can be expressed by

$$w^0 = \sum_{i=1}^{4} \boldsymbol{N}_i^0 \boldsymbol{q}_i \tag{8-173}$$

where

$$\left.\begin{aligned}
\boldsymbol{N}_i^0 &= [N_i^0 \quad N_{xi}^0 \quad N_{yi}^0]\\
\boldsymbol{q}_i &= [w_i \quad \psi_{xi} \quad \psi_{yi}]^{\mathrm{T}}
\end{aligned}\right\} \tag{8-174}$$

For element LFR1

$$\left.\begin{aligned} N_i^0 &= \frac{1}{8}(1+\xi_i\xi)(1+\eta_i\eta)(2+\xi_i\xi+\eta_i\eta-\xi^2-\eta^2) \\ N_{xi}^0 &= -\frac{a}{8}\xi_i(1+\xi_i\xi)(1+\eta_i\eta)(1-\xi^2)-\frac{a}{24}\xi_i\eta_i\eta(1-\eta^2) \\ N_{yi}^0 &= -\frac{b}{8}\eta_i(1+\xi_i\xi)(1+\eta_i\eta)(1-\eta^2)-\frac{b}{24}\xi_i\eta_i\xi(1-\xi^2) \end{aligned}\right\} \quad (8\text{-}175)$$

For element LFR2

$$\left.\begin{aligned} N_i^0 &= \frac{1}{8}(1+\xi_i\xi)(1+\eta_i\eta)(2+\xi_i\xi+\eta_i\eta-\xi^2-\eta^2) \\ N_{xi}^0 &= -\frac{a}{8}\xi_i(1+\xi_i\xi)(1+\eta_i\eta)(1-\xi^2) \\ N_{yi}^0 &= -\frac{b}{8}\eta_i(1+\xi_i\xi)(1+\eta_i\eta)(1-\eta^2) \end{aligned}\right\} \quad (8\text{-}176)$$

By the superposition of the displacement fields of the thin plate element given in Eq. (8-173) and the supplementary displacement fields of the thick plate element given in Eq. (8-172), the displacement fields of the thick plate element can be obtained. Then, the element stiffness matrices for two thin/thick plate elements can be derived according to the conventional procedure.

The above schemes have been further applied in references [18,19]. Since the generalized bubble displacement fields are introduced, the accuracy of the elements is improved, and the elements are insensitive to mesh distortion.

8.7.4 Numerical Examples

Example 8.5 The central deflection of simply-supported and clamped square plates (the side length is *L*) subjected to uniform load *q*. The Poisson's $\mu = 0.3$. The results by the elements LFR1 and LFR2 are given in Table 8.15.

It can be seen from Table 8.15 that, from thin plates to thick plates, elements LFR1 and LFR2 both provide results with high precision, but their derivation procedures are much simpler than that of the element in [16].

Example 8.6 Examine the convergence of elements LFR1 and LFR2 by refining the mesh. Tables 8.16 and 8.17 give the results for a thin square plate ($h/L = 10^{-3}$) and a thick square plate ($h/L = 0.3$) by using different meshes.

From Tables 8.16 and 8.17, it can be seen that, the elements LFR1 and LFR2 both have good convergence; when $h/L = 0.001$, the elements LFR1 and LFR2 will degenerate to be the thin plate elements LR12-2 and ACM, respectively.

Table 8.15 The central deflection coefficient of square plates subjected to uniform load $\Big/\left(\dfrac{qL^4}{100D}\right)$

h/L	Simply-supported				Clamped			
	Analytical	LFR1	LFR2	[16]	Analytical	LFR1	LFR2	[16]
10^{-11}	0.4062	0.4062	0.4105	0.4044	0.1265	0.1263	0.1290	0.1290
10^{-3}	0.4062	0.4062	0.4105	0.4044	0.1265	0.1263	0.1290	0.1293
10^{-2}	0.4062	0.4062	0.4106	0.4045	0.1265	0.1264	0.1293	0.1293
0.1	0.4273	0.4224	0.4304	0.4242	0.1499	0.1482	0.1522	0.1521
0.15	0.4536	0.4480	0.4566	0.4502	0.1798	0.1762	0.1802	0.1801
0.20	0.4906	0.4845	0.4933	0.4869	0.2167	0.2144	0.2183	0.2181
0.25	0.5379	0.5312	0.5401	0.5336	0.2675	0.2623	0.2661	0.2658
0.30	0.5956	0.5879	0.5968	0.5902	0.3227	0.3198	0.3235	0.3229
0.35	0.6641	0.6542	0.6631	0.6564	0.3951	0.3866	0.3902	0.3896

Note: a 10×10 mesh is used for the whole plate.

Table 8.16 Results for a thin plate ($h/L=10^{-3}$) by different meshes (uniform load)

Mesh for whole plate	Central deflection $\Big/\left(\dfrac{qL^4}{100D}\right)$				Moment $\Big/\left(\dfrac{qL^2}{10}\right)$			
	Simply-supported		Clamped		Simply-supported (central)		Clamped (mid-side)	
	LFR1	LFR2	LFR1	LFR2	LFR1	LFR2	LFR1	LFR2
2×2	0.3906	0.5063	0.1480	0.1480	0.6094	0.6602	– 0.3551	– 0.3551
4×4	0.4052	0.4328	0.1243	0.1403	0.5123	0.5217	– 0.4706	– 0.4761
8×8	0.4062	0.4129	0.1261	0.1304	0.4873	0.4892	– 0.5000	– 0.5028
16×16	0.4062	0.4079	0.1265	0.1275	0.4810	0.4814	– 0.5096	– 0.5104
Analytical	0.4062		0.1265		0.4789		– 0.5133	

Table 8.17 Results for a thick plate ($h/L=0.3$) by different meshes (uniform load)

Mesh for whole plate	Central deflection $\Big/\left(\dfrac{qL^4}{100D}\right)$				Moment $\Big/\left(\dfrac{qL^2}{10}\right)$			
	Simply-supported		Clamped		Simply-supported (central)		Clamped (mid-side)	
	LFR1	LFR2	LFR1	LFR2	LFR1	LFR2	LFR1	LFR2
2×2	0.5648	0.7081	0.3806	0.3806	0.8422	0.8395	– 0.4089	– 0.4089
4×4	0.5706	0.6201	0.3207	0.3377	0.5907	0.5739	– 0.4927	– 0.4604
8×8	0.5855	0.5992	0.3194	0.3250	0.5092	0.5031	– 0.4912	– 0.4604
16×16	0.5906	0.5942	0.3204	0.3219	0.4867	0.4850	– 0.4748	– 0.4546
Analytical	0.5956		0.3227		0.4789		– 0.4260	

References

[1] Reissner E (1995) The effect of transverse deformation on the bending of elastic plates. Journal of Applied Mechanics 12: A69 – 77

[2] Mindlin R D (1951) Influence of rotatory inertia and shear on flexural motion of isotropic elastic plates. Journal of Applied Mechanics 18: 31 – 38

[3] Hu HC (1984) Variational principles of theory of elasticity with applications. Science Press, Beijing

[4] Cen S, Long ZF (1998) A Mindlin triangular plate element with improved interpolation for the rotation and shear strain fields. Gong Cheng Li Xue/Engineering Mechanics 15(3): 1 – 14 (in Chinese)

[5] Zienkiewicz OC, Taylor RL, Too JM (1971) Reduced integration techniques in general analysis of plates and shells. International Journal for Numerical Methods in Engineering 3(2):275 – 290

[6] Hughes TJR, Cohen M, Haron M (1978) Reduced and selective integration technique in finite element analysis of plates. Nuclear Eng. and Design 46: 203 – 222

[7] Hinton E, Huang HC (1986) A family of quadrilateral Mindlin plate elements with substitute shear strain fields. Computers & Structures 23(3): 409 – 431

[8] Katili I (1993) A new discrete Kirchhoff-Mindlin element based on Mindlin-Reissner plate theory and assumed shear strain fields-part Ⅰ: An extended DKT element for thick-plate bending analysis. International Journal for Numerical Methods in Engineering 36: 1859 – 1883

[9] Cen S, Long ZF, Long YQ (1999) A Mindlin quadrilateral plate element with improved interpolation for the rotation and shear strain fields. Gong Cheng Li Xue/Engineering Mechanics 16(4): 1 – 15 (in Chinese)

[10] Cen S, Long ZF (1998) A new triangular generalized conforming element for thin-thick plates. Gong Cheng Li Xue/Engineering Mechanics 15(1): 10 – 22 (in Chinese)

[11] Cen S, Long YQ, Yao ZH, Chiew SP (2006) Application of the quadrilateral area coordinate method: a new element for Mindlin-Reissner plate. International Journal for Numerical Methods in Engineering 66(1): 1 – 45

[12] Long YQ, Fu XR (2002) Two generalized conforming quadrilateral thick plate elements based on analytical trial functions. Gong Cheng Li Xue/Engineering Mechanics 19(3): 10 – 15 (in Chinese)

[13] Chen YL, Cen S, Yao ZH, Long YQ, Long ZF (2003) Development of triangular flat-shell element using a new thin-thick plate bending element based on SemiLoof constrains. Structural Engineering and Mechanics 15(1): 83 – 114

[14] Long YQ, Bu XM, Long ZF, Xu Y (1995) Generalized conforming plate bending elements using point and line compatibility conditions. Computers & Structures 54(4): 717 – 723

[15] Fricker AJ (1986) A simple method for including shear deformation in thin plate elements. International Journal for Numerical Methods in Engineering 23: 1355 – 1366

[16] Long YQ, Xi F (1992) A universal method for including shear deformation in the thin plate elements. International Journal for Numerical Methods in Engineering 34: 171 – 177

[17] Long ZF (1992) Locking-free thick plate rectangular element. Gong Cheng Li Xue/ Engineering Mechanics 9(1): 88 – 93 (in Chinese)
[18] Cen S, Long ZF, Kuang WQ (1997) Improved thick plate elements by introducing generalized bubble displacement fields. In: Han DJ, Mo HH (eds) Computational Methods in Engineering and Science— Theory and Application (Proceedings of the Sixth EPMESC Conference). South China University of Technology Press, China, Guangzhou, pp517 – 522
[19] Cen S, Long ZF, Long YQ, Kuang WQ (1997) Two robust generalized conforming rectangular element for thin-thick plates. In: Han DJ, Mo HH (eds) Computational Methods in Engineering and Science— Theory and Application (Proceedings of the Sixth EPMESC Conference). South China University of Technology Press, China, Guangzhou, pp523 – 527
[20] Long ZF (1992) Triangular and rectangular plate elements based on generalized compatibility conditions. Computational Mechanics 10(3/4): 281 – 288
[21] Melosh RJ (1963) Basis for derivation of matrices for the direct stiffness method. AIAA Journal 1(7): 1631 – 1637